NASA Contractor Report 181725

SHAPE SENSITIVITY ANALYSIS OF FLUTTER RESPONSE OF A LAMINATED WING

Fred D. Bergen and Rakesh K. Kapania

VIRGINIA POLYTECHNIC INSTITUTE
AND STATE UNIVERSITY
Blacksburg, Virginia

Contract NAS1-18471
October 1988

National Aeronautics and
Space Administration

Langley Research Center
Hampton, Virginia 23665

Shape Sensitivity Analysis of Flutter Response of a Laminated Wing

by

Frederick D'Oench Bergen, Jr.

Rakesh K. Kapania

Aerospace and Ocean Engineering

(ABSTRACT)

A method is presented for calculating the shape sensitivity of a wing aeroelastic response with respect to changes in geometric shape. Yates' modified strip method is used in conjunction with Giles' equivalent plate analysis to predict the flutter speed, frequency, and reduced frequency of the wing. Three methods are used to calculate the sensitivity of the eigenvalue. The first method is purely a finite difference calculation of the eigenvalue derivative directly from the solution of the flutter problem corresponding to the two different values of the shape parameters. The second method uses an analytic expression for the eigenvalue sensitivities of a general complex matrix, where the derivatives of the aerodynamic, mass, and stiffness matrices are computed using a finite difference approximation. The third method also uses an analytic expression for the eigenvalue sensitivities but the aerodynamic matrix is computed analytically. All three methods are found to be in good agreement with each other. The sensitivities of the eigenvalues were used to predict flutter speed, frequency , and reduced frequency. These approximations were found to be in good agreement with those obtained using a complete reanalysis. However, it is recommended that higher order terms be used in the calculations in order to assure greater accuracy.

Acknowledgements

The authors would like to express their sincere thanks to Drs. Jean-Francois Barthelemy and Gary L. Giles at NASA, Langley Research Center for their helpful suggestions and contributions to this research. They would also like to thank Dr. R. T. Haftka and Dr. E. R. Johnson for their suggestions and comments.

Table of Contents

1.0 Introduction. 1

1.1 Introduction and Background 1

2.0 Structural Model 6

2.1 Introduction 6

2.2 Displacement Function 11

2.3 Energy Expressions 12

3.0 Aerodynamic Model 14

3.1 Aerodynamic Forces 14

3.2 Virtual Work 22

3.3 Flutter Analysis 26

4.0 Validation of Analysis Program 28

4.1 Introduction 28

4.2 Static Deflections 29

4.3 Free Vibration Analysis 30

4.4 Divergence and Flutter 39

5.0 Sensitivity Analysis **47**

5.1 Introduction 47

5.2 Eigenvalue Derivatives and Solution Procedures 48

5.3 Geometric Parameters 53

5.4 Analytic Derivatives 54

6.0 Conclusions and Suggestions for Future Work **78**

7.0 References 80

List of Illustrations

Figure 1. Local Coordinate System. 8

Figure 2. Possible Wing Box Geometry. 9

Figure 3. Wing Box Section Used. 10

Figure 4. Airfoil Geometry of a Typical Section. 17

Figure 5. Tip Deflection Comparison of Box Beam at Zero Sweep. 34

Figure 6. Comparison of Wing Geometries with Ref [21]. 35

Figure 7. Tip Deflection Comparison for Different Sweep Angles. 36

Figure 8. Variation of the Natural Frequencies with Fiber Angle. 37

Figure 9. Variation of Natural Frequencies with Sweep Angle. 38

Figure 10. Variation of Divergence with Sweep Angle. 41

Figure 11. Divergence and Flutter Speeds of 45 ° Sweptforward Box Beam. 42

Figure 12. Divergence and Flutter Speeds of 30 ° Sweptforward Box Beam. 43

Figure 13. Divergence and Flutter Speeds of Unswept Box Beam. 44

Figure 14. Divergence and Flutter Speeds of 30 ° Sweptback Box Beam. 45

Figure 15. Divergence and Flutter Speeds of 45 ° Sweptback Box Beam. 46

Figure 16. Flowchart of Semi-analytic Method 64

Figure 17. Flowchart of Analytic Method.....65

Figure 18. Flutter Frequency vs Surface Area. 66

Figure 19. Flutter Speed vs Surface Area. 67

Figure 20. Reduced Frequency vs Surface Area.....68

Figure 21. Flutter Frequency vs Aspect Ratio. 69

Figure 22. Flutter Speed vs Aspect Ratio..... 70

Figure 23. Reduced Frequency vs Aspect Ratio. 71

Figure 24. Flutter Frequency vs Taper Ratio.....72

Figure 25. Flutter Speed vs Taper Ratio. 73

Figure 26. Reduced Frequency vs Taper Ratio.....74

Figure 27. Flutter Frequency vs Sweep Angle 75

Figure 28. Flutter Speed vs Sweep Angle. 76

Figure 29. Reduced Frequency vs Sweep Angle.....77

List of Tables

Table 1. Abscissas and Weight in Gaussian Quadrature, n = 15. 25

Table 2. Comparisons of Tip Deflections for Different Aspect Ratios..... 32

Table 3. Comparison of Natural Frequencies for Different Aspect Ratios..... 33

Table 4. Comparison of Finite Difference Step Sizes 62

Table 5. Comparison of Eigenvalue Derivatives. 63

List of Symbols

a.....Distance between Reference Line and Midchord

a', c, e, f, g' .....Coefficients to Define Wing Geometry

$[A]$, A_{ij}.....Aerodynamic Matrix

A_{ah}, $A_{a\alpha}$, $A_{a\tau}$.....Aerodynamic Coefficient Used in Moment Expression

A_{ch}, $A_{c\alpha}$, $A_{c\tau}$.....Aerodynamic Coefficient Used in Lift Expression

a_{cn}.....Distance to Aerodynamic Center

AR.....Aspect Ratio of Half Wing

b.....Halfchord Defined Perpendicular to Reference Line

B.....Span along Half Wing

[B].....General Complex Matrix

$B_{ch}, B_{c\theta}$..... Aerodynamic Coefficients used in Lift Expression

$B_{ah}, B_{a\theta}$..... Aerodynamic Coefficients used in Moment Expression

$C_{l\alpha}$.....Lift Curve slope of Free Stream Elastic Axis

$C_{l\alpha,n}$.....Lift Curve slope defined Perpendicular to Reference Axis

$C(k_n)$.....Theodorsen Circulation Function

C_{mn}.....Coefficients of Deflection Equation

C_r .....Chord Root

crd(i).....Chord Length Perpendicular to Reference Line

C_t .....Chord Tip

δC_i .....Virtual Displacement in i^{th} Generalized Coordinate

D_{ij} .....Bending Stiffness Coefficient

E .....Total Energy

E_{11} .....Modulus of Elasticity in Principle Direction

E_{22} .....Modulus of Elasticity in Secondary Direction

e_r, e_l .....Right and Left Eigenvectors, respectively

g.....Damping Coefficient

G_{12} .....Shear modulus

h .....Deflection of Reference Line

δh.....Virtual Displacement

$H(x,y)$ .....Depth of Box Section

H_{mn} .....Coefficient Used to Model Depth of Box Section

[I].....Identity Matrix

[K].....Stiffness Matrix

k_n .....Reduced Frequency

L .....Lift Forces, Defined along Reference Line

[M].....Mass Matrix

m .....mass per unit area

Q_d.....Downwash Distribution

Q_i .....Generalized Forces

S .....Surface Area of Half Wing

$t(x,y)$ .....Thickness Distribution of Laminate

t_{mn} .....Coefficient to Model Thickness

tp .....Taper Ratio

T .....Kinetic Energy

U .....Strain Energy

V_n .....Flutter Velocity Perpendicular to Reference Line

$W(x,y)$ .....Deflection Shape Function

W .....Transverse Velocity

δW_{nc} .....Work Due to the Non-conservative Forces

x .....Global Coordinate in Chordwise Direction

x' .....Coordinate Defined Perpendicular to Reference Line

$\tilde{x}$ .....Coordinate Position of the Reference Line

y .....Global Coordinate in Spanwise Direction

$\tilde{y}$ .....Coordinate Position of the Reference Line

Z .....Global Coordinate Positive Upward

Z_c .....Distance to Reference Line

Z_{mn} .....Coefficient to Define Mid-camber Surface

Greek Symbols.

σ .....Local Bending Slope of Reference Line

τ ..... Local Rate of Change of Twist

η .....Local Coordinate in Spanwise Direction

ζ .....Local Coordinate in Chordwise Direction

ρ .....Air Density

ρ_{mat} .....Material Density

ω ..... Frequency of Vibration

θ ..... Rotation Angle Measured Perpendicular to Reference Axis

$\delta\theta$ ..... Virtual Rotation of i^{th} Generalized Coordinate

γ ..... Displacement Function

$\bar{\gamma}$ ..... Displacement Function Defined Perpendicular to Reference Axis

ν_{12} ..... Possion's Ratic

λ ..... Eigenvalue

Λ ..... Midchord Sweep Angle

Superscripts

$_{,x}$ ..... Derivative with respect to global x

$_{,y}$ ..... Derivative with respect to global y

^{t} ..... Transpose

$[\,]$ ..... Matrix

$\{\}$ ..... Vector

$\frac{\partial}{\partial p_i}$ ..... Partial Derivative with respect to Shape Parameter

$\frac{d}{dp_i}$ ..... Total Derivative with respect to Shape Parameter

$\frac{\partial}{\partial k_n}$ ..... Partial Derivative with respect to Reduced Frequency

$\frac{d}{dk_n}$ ..... Total Derivative with respect to Reduced Frequency

1.0 Introduction.

1.1 Introduction and Background

Flutter, an aeroelastic instability, is a self-sustaining oscillation that involves the coupling of inertial, elastic, and aerodynamic forces. Tail flutter was the earliest documented case of dynamic aeroelastic instability. It was discovered on the twin-engined Handley Page 0/400 Bomber at the beginning of World War I that the fuselage and tail had two principal modes of vibration. In the first mode, the elevators oscillated about their hinges 180 degrees out of phase, because the elevators were not attached by a torque tube. In the second mode, the fuselage oscillated in torsion. The coupling between these two modes resulted in a self-sustained oscillation [1].

Modern aircrafts are subjected to numerous types of flutter phenomena. Classical flutter is associated with potential flow and involves coupling of two or more degrees of freedom. Nonclassical flutter is concerned with oscillations due to boundary layer effects, such as separeted flow and reattaching flows. Nonclassical flutter is more difficult to

analyze from a theoretical standpoint. Only classical flutter will be analyzed in this presentation.

Flutter analysis capablities have been available for well over four decades. Loring [2] developed a general approach to the flutter problem in 1941. Yates [3] developed a modified strip analysis to analyze flutter characteristics for finite-span swept and unswept wings at subsonic and supersonic speeds in 1958. This method is still used today to calculate the lift and moment forces. For example, Landsberger and Dugundji [4] used these expressions, with a modification for camber effects given by Spielberg [5], to study the flutter and divergence of a composite plate. The present day computers allow still more complex aerodynamic programs to be developed and used. To name a few, the unsteady vortex-lattice method developed by Strganac and Mook [6], the double lattice method developed by Waldman [7], and the MCAERO code developed by Hawk and Bristow [8].

The dynamics of any physical system is important from a designer's view point. The onset of flutter in a modern aircraft will involve large oscillatory distortions of the structural components. Therefore, it would be advantageous to the designer to have a tool which can be used to predict the changes in flutter with the changes in basic shape parameters.

Sensitivity analysis was first recognized as a useful tool for assessing the effects of changing parameters in mathmatical models of control systems. The gradient based mathematical programming method used in optimal control and structural optimization furthered the development of sensitivity derivatives, because sensitivity derivatives are used in search directions to find optimum solution [9,10,11,12]. Inefficient optimization programs lead to further interest in efficient calculation of sensitivity derivatives. As a

result, sensitivity analysis has become a versatile design tool, rather than just an instrument of optimization programs [13].

Shape sensitivity analysis of any physical system under aeroelastic loads can be important from different points of view: 1) to understand and predict the system's response and 2) to optimize the response of the system for a set of physical constraints. In order to predict or optimize the response the sensitivity derivatives must be calculated. This can be done by a finite difference calculation or analytical calculation of the sensitivity derivatives. Analytical sensitivity analysis has found increased interest in engineering design. The analytical derivatives eliminate the uncertainty in the choice of step size, which if too large can lead to truncation errors and if too small can lead to ill-conditioning.

Adelman and Haftka [13] have shown that structural sensitivity analysis has been available for over two decades. Structural sensitivity analysis has been sufficient in the past because sizing variables such as plate thickness and cross-sectional areas effect the mass and stiffness properties of the airframe but, not its basic geometry. Therefore, aerodynamic sensitivity analysis capability has been limited in development until recently.

For example, Rudisill and Bhatia [14] developed expressions for the analytical derivatives of the eigenvalues, reduced frequency and flutter speed with respect to structural parameters for use in minimizing the total mass. However, this method is limited because the structural parameters are sizing variables such as cross-sectional areas, plate thickness and diameters of spars.

Pedersen and Seyranian [15], examined the change in flutter load as a function of change in stiffness, mass, boundary conditions or load distribution. They showed how sensitivity

analysis can be performed without any new eigenvalue analysis. The solution to the main and an adjoint problem provide all the necessary information for evaluating sensitivities. Their paper mainly focuses on column and beam critical load distributions.

Hawk and Bristow [8] developed aerodynamic sensitivity analysis capabilities in subcritical compressible flow. They first analyzed a baseline configuration, and then calculated a matrix containing the partial derivatives of the potential at each control point with respect to each known geometric parameter by applying a first-order expansion to the baseline configuration. The matrix of partial derivatives is used in each iteration cycle to analyze the perturbed geometry. However, this analysis only handles chordwise perturbation distributions, such as changes in camber, thickness and twist. A new approach, which is still under development, has been proposed by Yates [16] that considers general geometric variations, including planform, for subsonic, sonic and supersonic unsteady, nonplanar lifting-surface theory.

Barthelemy and Bergen [17] explored the analytical shape sensitivty derivatives of a wing static aeroelastic response. They found that the second derivatives of the wing's aeroelastic characteristics, such as section lift, angle of attack , rolling moment, induced drag, and divergence dynamic pressure, for subsonic subcritical flow, with respect to geometric parameters are small enough to be well approximated by sensitivity based linear approximations. These approximations are valid within a range that are useful to the designer in the initial design phase.

This work is an extension of previous work preformed by Barthelemy and Bergen [17], and details the theoretical and computational derivation of a method to obtain the sensitivity of a wing flutter response to changes in its geometry. Specifically, the objective is to determine the derivatives of flutter speed and frequency with respect to wing area,

aspect ratio, taper ratio, and sweep angle. Chapter 2 gives a brief description of the structural formulation which was originally formulated at the NASA Langley Reasearch Center by Giles [18]. The program is based upon a Raleigh-Ritz formulation in which the displacement functions are made up of polynomial expressions. The aerodynamic formulation is presented in Chapter 3. The expression for lift and moment are derived from potential flow theory and have been modified to account for finite span. In Chapter 4, the formulation is validated using examples found in other works. Once there is sufficient confidence in the flutter speed prediction capablities, it is shown that the sensitivity analysis will predict the flutter speed for changes in the structural parameters. Three different approaches are used to obtain the sensitivity of the flutter speed, frequency, and reduced frequency to various shape parameters. These include:

(i) a purely numerical approach using the finite difference method;

(ii) a semi-analytical method that uses an analytic expression given by Murthy and Haftka [19], for calculating the sensitivity of the eigenvalues of a generalized eigenvalue problem and a finite difference approximation of the derivatives of the aerodynamic, mass and stiffness matrices with respect to the geometric parameters; and

(iii) an analytic approach that uses the analytic expression for calculating the sensitivity of the eigenvalues and an analytically derived expression for the sensitivity of the aerodynamic matrix with respect to geometric parameters.

Chapter 6 gives conclusions and suggestions for future work.

2.0 Structural Model

2.1 Introduction

This chapter presents the structural formulation which was originally programmed by Giles [18]. The program is based upon a Ritz solution technique using the the energy functionals for a laminated plate which includes the bending and stretching of the reference surface. This program is capable of analyzing unsymmetric wing box sections arising from airfoil camber, laminate sequences, or different thicknesses in upper and lower cover skins. Thermal loadings can be represented as temperature distributions over the planform of the cover skins.

The aerodynamic formulation restricts the chordwise length to remain straight during oscillations, therefore only high aspect ratio wings will be analyzed in this presentation. Only bending and torsional deformations are considered in this analysis procedure. In the theory of plates, the Kirchhoff assumption is made that lines normal to the reference plane remain straight and normal after deformations.

The planform geometry of the wing is represented by a trapezoidal segment. To represent cranked wing boxes, multiple trapezoidal segments can be defined. Each segment has a separate local coordinate system. The local coordinates are nondimensional such that ξ refers to a fraction of the chord and η a fraction of the span as shown in Figure 1.

Figure 2 illustrates a possible geometry of the wing box and coordinate system. The mid-camber surface is measured from a reference plane. The distance, Z_c, is represented as a polynomial in the global coordinates x and y.

$$Z_c(x,y) = z_{00} + z_{10}x + z_{20}x^2 + z_{01}y + \ldots + z_{mn}x^m y^n \qquad [2.1.1]$$

The depth of the wing box, H(x,y) is measured from the midchord surface and the thickness t(x,y) of each laminate is also defined by polynomial expressions x and y. The expressions for the depth and thickness are:

$$H(x,y) = H_{00} + H_{10}x + H_{20}x^2 + H_{01}y + \ldots + H_{mn}x^m y^n \qquad [2.1.2]$$

$$t(x,y) = t_{00} + t_{10}x + t_{20}x^2 + t_{01}y + \ldots + t_{mn}x^m y^n \qquad [2.1.3]$$

In the present formulation, the depth of the wing box and thickness of the skins is assumed to be constant throughout. The coefficients of equations (2.1.2) and (2.1.3) are:

$$H_{00} = .100 \quad meters \qquad t_{00} = .002 \quad meters$$

$$H_{mn} = 0.0 \qquad t_{mn} = 0.0 \qquad m = 1,\ldots,5 \qquad n = 1,\ldots,5$$

The wing box used for this presentation is shown in Figure 3. The box section chordline is straight, therefore $Z_c(x,y)$ is zero for this presentation.

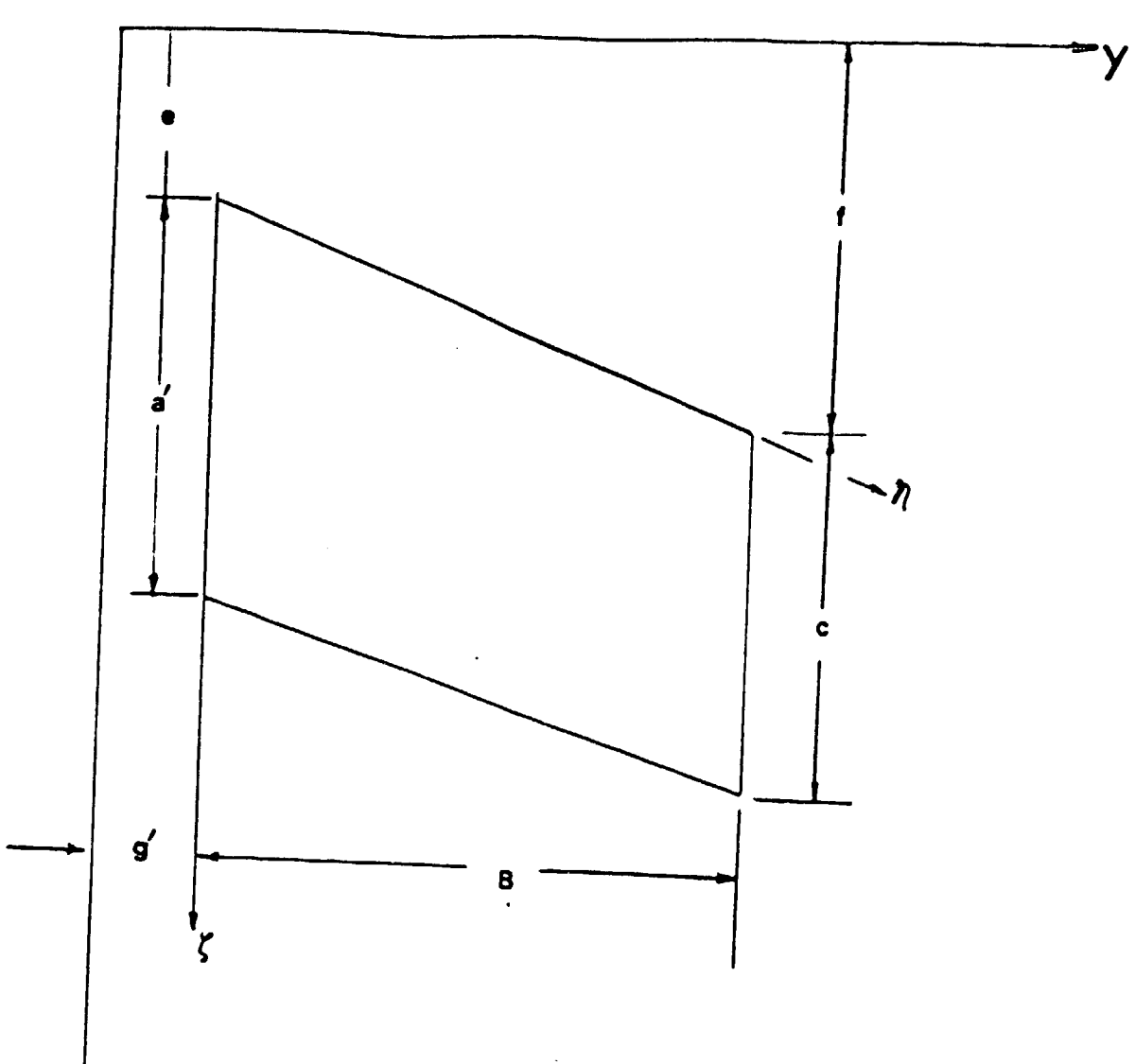

Figure 1 Local Coordinate System

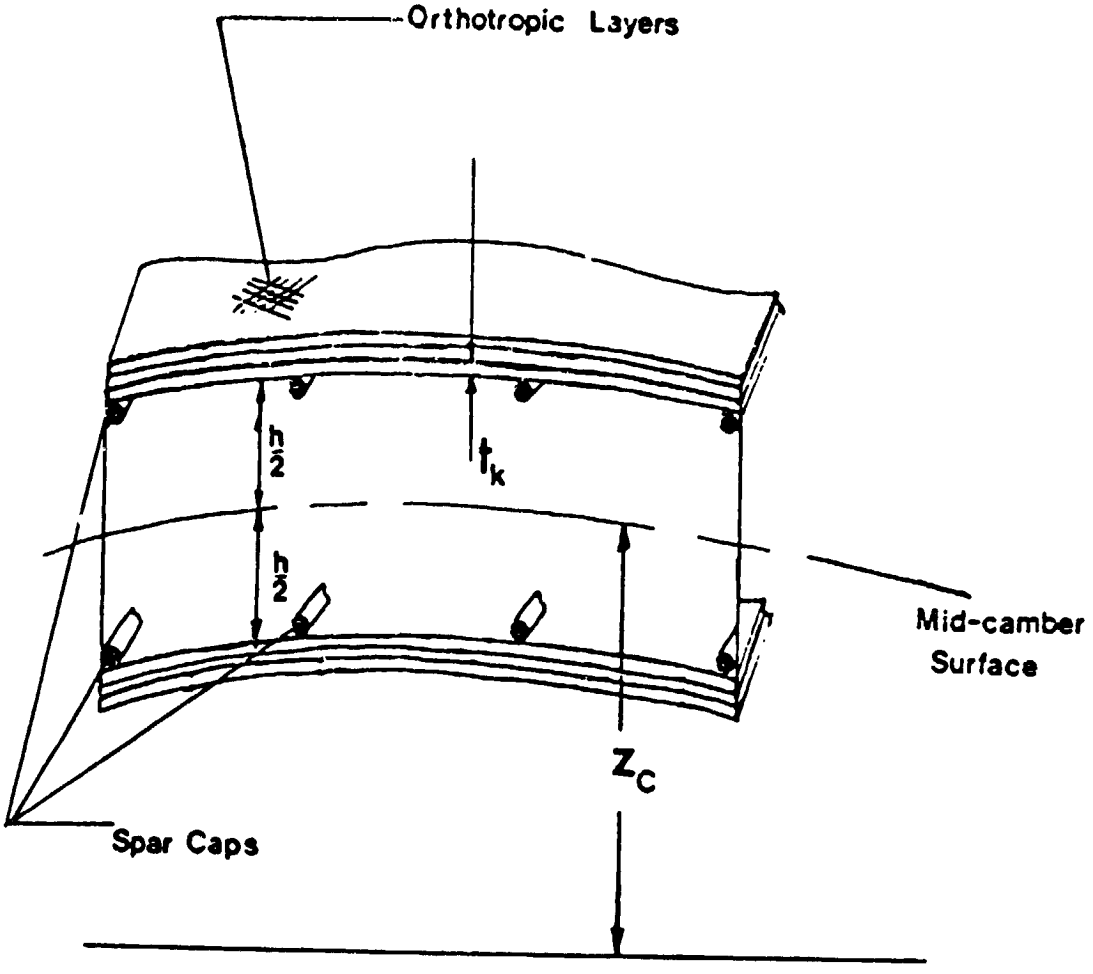

Figure 2 Possible Wing Box Geometry

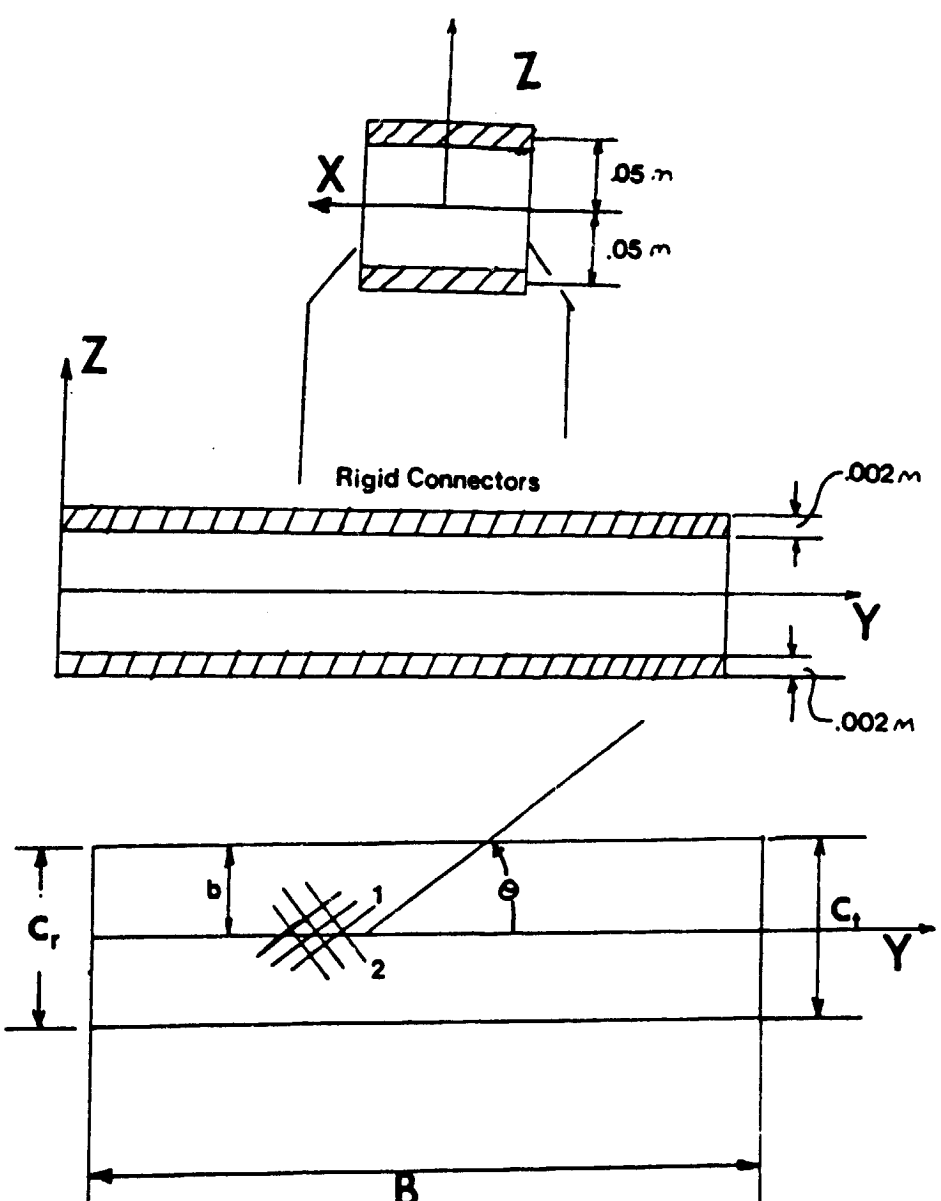

Figure 3 Wing Box Section Used

2.2 *Displacement Function*

The Rayleigh-Ritz formulation assumes a deflection shape for the wing structure. This deflection shape is a linear combination of n assummed displacement functions. The assumed displacement functions are specified as products of polynomial x-direction and y-direction global coordinates. The deflection equation can be written as:

$$W(x,y) = \sum_{n=0}^{N} \sum_{m=2}^{M} C_{nm} \left(\frac{x}{x_{max}}\right)^n \left(\frac{y}{y_{max}}\right)^m \qquad [2.2.1]$$

where N is restricted to five terms and M is restricted to six terms in order to prevent numerical difficulties in the manipulation of the matrices. $W(x,y)$ is the transverse deflection of the reference line , and C_{nm} the set of unknown coefficients.

The deflection equation can also be written as:

$$W(x,y) = \sum_{i=1}^{np} \gamma_i (x,y)\ C_i \qquad [2.2.2]$$

where γ_i (x, y) is the nondimensional displacement function and np is N times M. All the assumed displacement functions satisfy the geometric boundary conditions for a cantilever plate. The constants x_{max} and y_{max} are defined in magnitude as the root chord and span respectively. The displacement functions are nondimensional quantities in order to prevent numerical difficulties in manipulation of the matrices.

2.3 *Energy Expressions*

The strain energy U for a symmetric anisotropic laminate is given as:

$$U = \frac{1}{2}\iint_A \{D_{11}W_{,xx}^2 + 2D_{12}W_{,xx}W_{,yy} + D_{22}W_{,yy}^2$$

$$+ 4D_{16}W_{,xy}W_{,xx} + 4D_{26}W_{,xy}W_{,yy} + 4D_{66}W_{,xy}^2 \}dA \qquad [2.3.1]$$

where a comma denotes partial differentiation and D_{ij} are the bending stiffness terms. The kinetic energy T for the plate is:

$$T = 1/2\iint_A m\dot{W}^2 dA \qquad [2.3.2]$$

where m is the distributed mass per unit area $\dot{W}$ is the transverse velocity at x and y, and A is the area of the plate.

The Ritz solution procedure is used to determine the numerical values of the set of unknown coefficients, C_i's. To use the Ritz solution procedure, and to integrate these equations the global x and y were transformed into a local system. This was achieved by the following transformation.

$$x = e + a'\xi + (f - e)\eta + (c - a')\eta\xi \qquad [2.3.3]$$

$$y = g' + B\eta \qquad [2.3.4]$$

The coefficients a', B, c, e, f, g' are dimensions of the local coordinate system as shown in Figure 1.

The Ritz solution procedure is based upon the second variational priniciple. The second variational priniciple states that the total energy of the structure can be written in terms of any kinematically admissible function. If the total energy, $E(\tilde{y})$, in terms of the kinematically admissible function $\tilde{y}$, is stationary at $\tilde{y} = y$ with $E(y) = 0$, then the function represents the real modes of the structure. If the function represents the real modes of the structure then it can be used as a valid approximation to the exact solution. The total energy of the structure can be written as:

$$E = U - T \qquad [2.3.5]$$

The extremum principle states that the energy is stationary with respect to C_i i.e. $\frac{\partial E}{\partial C_i} = 0$. This produces a system of n simultaneous equations. In matrix form then the equations are expressed as:

$$[[K] - \omega^2[M]]\{C\} = \{0\} \qquad [2.3.6]$$

where [K] and [M] are the stiffness and mass matrices resulting from the partial differentiation of the potential and kinetic energies, recpectively, with respect to the generalized coordinates.

3.0 Aerodynamic Model

3.1 Aerodynamic Forces

This chapter presents the formulation of the aerodynamic coefficient matrix. An incompressible, 2-dimensional, unsteady strip theory was used to calculate the aerodynamic coefficients. This method was first developed by Barnby, et. al., [20] and was modified by Yates [16] to include the effects of finite span. Lift and moment forces are defined along the midchord and acting upon sections perpendicular to this midchord line (called the reference line hereafter).

The flow field is represented by a uniform stream (non-circulatory component) superposed by the disturbance-velocity distribution (circulatory component) which will model the effect of the position and motion of the wing. It is modeled such that the condition of tangential flow at the wing surface is met.

The position of each point of the segment taken perpendicular to the reference line is:

$$Z = h + x'\theta \qquad [3.1.1]$$

Where h is the deflection of the midchord, positive up, θ is the rotation of a section measured perpendicular to the midchord positive leading edge down, and x' is the perpendicular distance from the reference line, measured positive back.

The lift and moment forces are written in terms of a circulatory and non-circulatory components. As taken from Yates' modified strip analysis [3], the lift force (positive up) per unit length of the wing, is given as:

$$L = -\pi\rho b^2[\ddot{h} + V_n\dot{\theta} + V_n\dot{\sigma}\tan\Lambda - ba(\ddot{\theta} + V_n\dot{\tau}\tan\Lambda)]_{nc}$$

$$-[C_{l\alpha,n}\rho V_n bC(k_n)\mathcal{Q}_d]_c \qquad [3.1.2]$$

where subscript nc indicates the noncirculatory component and c indicates the circulatory component. The air density is ρ, b is the halfchord, V_n is the air speed measured perpendicular to the midchord. $C_{l\alpha,n}$ is the section lift coefficient which is constant along the span, Λ is the midchord sweep angle, and a is the off-set of the reference line from the midchord line, assumed to be zero in this presentation. The local bending slope of the reference axis is represented by σ and the local rate of change of twist is represented by τ. $C(k_n)$ is Theoderson's circulation function. The reduced frequency, k_n is a measure of the amount of circulation in the flow field and is used in the circulation function and is given as [10]:

$$C(k_n) = 1 - \frac{0.165}{1 - \frac{0.0455}{k_n}i} - \frac{0.335}{1 - \frac{0.3}{k_n}i} \qquad [3.1.3]$$

Similarly, the expression for the moment M, per unit length about the midchord (positive leading edge down) is :

$$M = -\pi\rho b^4[(\frac{1}{8} + a^2)(\ddot{\theta} + V_n\dot{\tau}\tan\Lambda) + \pi\rho b^2 V_n(\dot{h} + V_n\sigma\tan\Lambda) + \pi\rho b^3 a(\ddot{h} + V_n\dot{\sigma}\tan\Lambda)$$

$$+ \pi\rho V_n^2 b^2(\theta - ab\tau\tan\Lambda)]_{nc}$$

$$[-2\pi\rho V_n b^2[\frac{1}{2} - (a - a_{cn})C(k)\frac{C_{l_\alpha, n}}{2\pi}]Q_d]_c \qquad [3.1.4]$$

where a_{cn} is the distance to the aerodynamic center from the reference line, and Q_d is the downwash distribution defined by:

$$Q_d = \dot{h} + V_n\theta + V_n\sigma\tan\Lambda + b(\frac{C_{l_\alpha, n}}{2\pi} + a_{cn} - a)(\dot{\theta} + V_n\tau\tan\Lambda) \qquad [3.1.5]$$

The airfoil geometry with typical dimensions is shown in Figure 4.

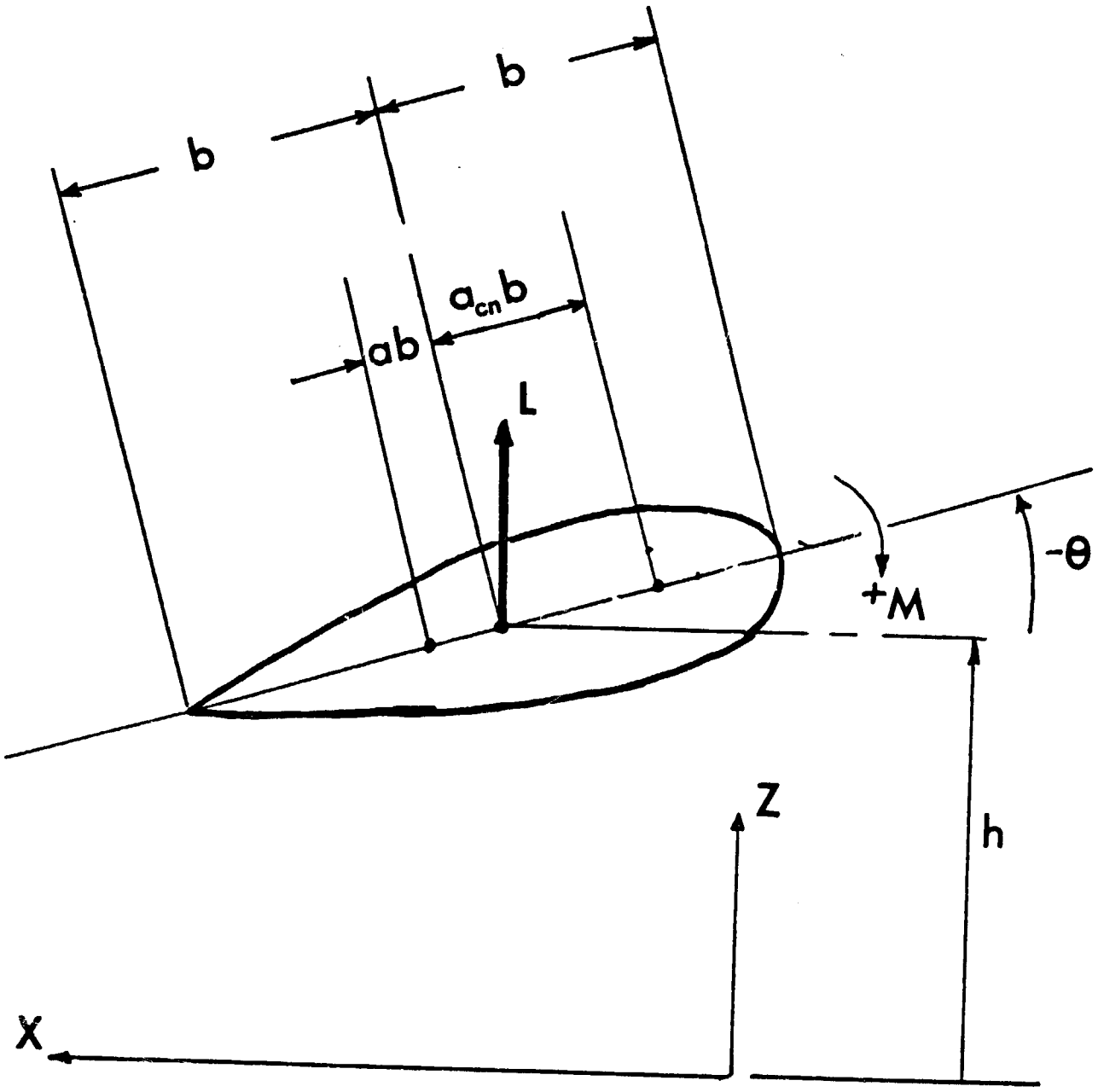

Figure 4 Airfoil Geometry of a Typical Section

The lift and moment forces can be reduced to the following expressions assuming the wing is undergoing infinitesimal harmonic oscillations about its steady-state position [20].

$$L = -\pi\rho b^3\omega^2(B_{ch}h + B_{c\theta}\theta) \qquad [3.1.5]$$

$$M = -\pi\rho b^4\omega^2(B_{ah}h + B_{a\theta}\theta) \qquad [3.1.6]$$

The coefficients $B_{ch}, B_{c\theta}, B_{ah}$, and $B_{a\theta}$ are defined as:

$$B_{ch} = \frac{1}{b}A_{ch} - \frac{i\sigma}{k_n h}A_{ch}\tan\Lambda \qquad [3.1.7]$$

$$B_{c\theta} = A_{c\alpha} + \frac{\tau}{\theta}bA_{c\tau}\tan\Lambda \qquad [3.1.8]$$

$$B_{ah} = \frac{1}{b}A_{ah} - \frac{i\sigma}{k_n h}A_{ah}\tan\Lambda \qquad [3.1.9]$$

$$B_{a\theta} = A_{a\alpha} + \frac{\tau}{\theta}bA_{a\tau}\tan\Lambda \qquad [3.1.10]$$

and;

$$A_{ch} = -1 + \frac{2iC(k_n)C_{l\alpha,n}}{k_n 2\pi} \qquad [3.1.11]$$

$$A_{c\alpha} = a + \frac{i}{k_n} + \frac{2iC(k_n)C_{l\alpha,n}}{k_n 2\pi}(1-2a) + \frac{2C(k_n)C_{l\alpha,n}}{k_n^2 2\pi} \qquad [3.1.12]$$

$$A_{c\tau} = \frac{ia}{k_n} + \frac{2C(k_n)C_{l\alpha,n}}{k_n 2\pi}(-a_{cn} - a) \qquad [3.1.13]$$

$$A_{ah} = a - \frac{2iC(k_n)C_{l\alpha,n}}{k_n 2\pi}(-a_{cn} + a) \qquad [3.1.14]$$

$$A_{a\alpha} = -\frac{1}{8} - a^2 + \frac{i}{k_n}(\frac{1}{2} - a)$$

$$-\frac{2C(k_n)C_{l\alpha,n}}{k_n^2 2\pi}(a_{cn} - a) - \frac{2iC(k_n)C_{l\alpha}sub,n}{k_n 2\pi}(a_{cn}^2 - a^2) \qquad [3.1.15]$$

$$A_{a\tau} = -\frac{i}{k_n}[-\frac{3}{8} + \frac{i}{2k_n} - (a_{cn}^2 - a^2)A_{ch}] \qquad [3.1.16]$$

The bending deflection, h, and the torsional deflection,θ , are defined along the reference line -- the midchord.

Special attention must be made when expressing the quantities which relate the aerodynamic and structural models. The aerodynamic forces and displacements are derived in terms of sections perpendicular to the reference line. The displacement functions (see Chapter 2) and their derivatives define rotations parellel to the free stream flow. In order to be consistent in the formulation, $\gamma_{i,x}$, $\gamma_{i,y}$, and $\gamma_{i,xy}$ must be transformed to define θ, τ, and σ in the plane perpendicular to the reference line. These transformations are as follows:

$$\theta(\tilde{x}, \tilde{y}) = \sum_{i=1}^{np} C_i(\gamma_{i,x}(\tilde{x}, \tilde{y})\cos\Lambda - \gamma_{i,y}(\tilde{x}, \tilde{y})\sin\Lambda) \qquad [3.1.17]$$

$$\tau(\tilde{x}, \tilde{y}) = \sum_{i=1}^{np} C_i(\gamma_{i,x}(\tilde{x}, \tilde{y})\sin\Lambda + \gamma_{i,y}(\tilde{x}, \tilde{y})\cos\Lambda) \qquad [3.1.18]$$

$$\sigma(\tilde{x},\tilde{y}) = \sum_{i=1}^{np} C_i(\gamma_{i,xx}(\tilde{x},\tilde{y})\cos\Lambda\sin\Lambda$$

$$+\gamma_{i,xy}(\tilde{x},\tilde{y})(\cos^2\Lambda - \sin^2\Lambda) - \gamma_{i,yy}(\tilde{x},\tilde{y})\cos\Lambda\sin\Lambda) \qquad [3.1.19]$$

Here the superscripts~ represent the fact that x, y are not any arbitrary values of x and y, but $\tilde{x}$, $\tilde{y}$ are the coordinates of the reference line in x and y. Futhermore:

$$\tilde{x} = \tilde{y}\tan\Lambda \qquad [3.1.20]$$

Therefore h, θ, τ, and σ are functions of $\bar{y}$ only, where $\bar{y}(=\frac{\tilde{y}}{\cos\Lambda})$ is the distance of the point $\tilde{x},\tilde{y}$ from the origin along the reference line. For simplicity, h, θ, τ, and σ can be written as:

$$h(\bar{y}) = \sum_{i=1}^{np} C_i\ \bar{\gamma}(\bar{y}) \qquad [3.1.21]$$

$$\theta(\bar{y}) = \sum_{i=1}^{np} C_i\ \bar{\gamma}_{i,\bar{x}}(\bar{y}) \qquad [3.1.22]$$

$$\sigma(\bar{y}) = \sum_{i=1}^{np} C_i\ \bar{\gamma}_{i,\bar{y}}(\bar{y}) \qquad [3.1.23]$$

$$\tau(\bar{y}) = \sum_{i=1}^{np} C_i\ \bar{\gamma}_{i,\overline{xy}}(\bar{y}) \qquad [3.1.24]$$

The lift and moment forces can then be written in terms of the displacement functions $\bar{y}_i(\bar{y})$ and the unknown coefficients, C_i. Based upon equations 3.1.5, 3.1.6, and 3.1.17-3.1.24, the lift and moment can be written as:

$$L = -\pi\rho b^3\omega^2 \left\{ \frac{1}{b}\sum_{m=1}^{np} \bar{y}_m(\bar{y})\, C_m - \frac{i}{k_n}\tan\Lambda \sum_{m=1}^{np} \bar{y}_{m,\bar{y}}(\bar{y})\, C_m \right\} A_{ch}$$

$$+ A_{c\alpha}\sum_{m=1}^{np} \bar{y}_{m,\bar{x}}(\bar{y})\, C_m + bA_{c\tau}\tan\Lambda \sum_{m=1}^{np} \bar{y}_{m,\overline{xy}}(\bar{y})\, C_m \qquad [3.1.25]$$

$$M = -\pi\rho b^4\omega^2 \left\{ \frac{1}{b}\sum_{m=1}^{np} \bar{y}_m(\bar{y})\, C_m - \frac{i}{k_n}\tan\Lambda \sum_{m=1}^{np} \bar{y}_{m,\bar{y}}(\bar{y})\, C_m \right\} A_{ah}$$

$$+ A_{a\alpha}\sum_{m=1}^{np} \bar{y}_{m,\bar{x}}(\bar{y})\, C_m + bA_{a\tau}\tan\Lambda \sum_{m=1}^{np} \bar{y}_{m,\overline{xy}}(\bar{y})\, C_m \qquad [3.1.26]$$

Having obtained the lift and moment forces, in terms of the displacement function and unknown coefficients, attention must be focused on the principle of virtual work since these forces are non-conservative. At this point forward, $\bar{y}(\bar{y})$ will be represented as $\bar{y}$ for ease in derivations.

3.2 *Virtual Work*

The lift and moment forces are non-conservative forces, therefore the principle of virtual work must be employed. The definition of virtual work gives:

$$\delta W_{nc} = \int_0^l L\delta h d\bar{y} + \int_0^l M\delta\theta d\bar{y} = \sum_{j=1}^{n} Q_j \delta C_j \qquad [3.2.1]$$

where δh, and $\delta\theta$ are the virtual displacements and Q_j are the generalized forces. The virtual displacements are defined as:

$$\delta h = \sum_{j=1}^{np} \bar{\gamma}_j \delta C_j \qquad [3.2.2]$$

$$\delta\theta = \sum_{j=1}^{np} \bar{\gamma}_{l,\bar{x}} \delta C_j \qquad [3.2.3]$$

The virtual work can be expressed in terms of generalized forces and displacements as:

$$\delta W_{nc} = \sum_{i=1}^{np} Q_i \delta C_i \qquad [3.2.4]$$

This can be written as:

$$\delta W_{nc} = -\sum_{j=1}^{np}\Big[\int_0^l \pi\rho b^3\omega^2 \sum_{i=1}^{np}\Big[\frac{1}{b}(\bar{\gamma}_i\ \bar{\gamma}_j)C_i - \frac{i}{k_n}\tan\Lambda(\bar{\gamma}_{i,\bar{y}}\ \bar{\gamma}_j)C_i\Big]A_{ch}$$

$$+ (\bar{\gamma}_{i,\bar{x}}\ \bar{\gamma}_j)C_iA_{c\alpha} + b\tan\Lambda(\bar{\gamma}_{i,\overline{xy}}\ \bar{\gamma}_j)C_iA_{c\tau} \quad d\bar{y}\delta C_j$$

$$-\int_0^l \pi\rho b^4\omega^2 \sum_{i=1}^{np}\Big[\frac{1}{b}(\bar{\gamma}_i\ \bar{\gamma}_{j,\bar{x}})\,C_i - \frac{i}{k_n}\tan\Lambda(\bar{\gamma}_{i,\bar{y}}\ \bar{\gamma}_{j,\bar{x}})\,C_i\Big]A_{ah}$$

$$+ \bar{\gamma}_{i,\bar{x}}\ \bar{\gamma}_{j,\bar{x}}\,C_iA_{a\alpha} + b\tan\Lambda(\bar{\gamma}_{i,\overline{xy}}\ \bar{\gamma}_{j,\bar{x}})C_iA_{a\tau}\ \Big]\ d\bar{y}\delta C_j \qquad [3.2.5]$$

The generalized forces are defined as:

$$Q_j = \omega^2\sum_{i=1}^{np}A_{ji}\ \ C_i \qquad [3.2.6]$$

The aerodynamic matrix then becomes:

$$A_{ji} = -\int_0^l \pi\rho b^3\{\Big[\frac{1}{b}(\bar{\gamma}_i\ \bar{\gamma}_j) - \frac{i}{k_n}\tan\Lambda(\bar{\gamma}_{i,\bar{y}}\ \bar{\gamma}_j)\Big]A_{ch}$$

$$+ \bar{\gamma}_{i,\bar{x}}\,\bar{\gamma}_jA_{c\alpha} + b\tan\Lambda(\bar{\gamma}_{i,\overline{xy}}\ \bar{\gamma}_j)A_{c\tau}\}\ d\bar{y}$$

$$-\int_0^l \pi\rho b^4\{\Big[\frac{1}{b}(\bar{\gamma}_i\ \bar{\gamma}_{j,\bar{x}}) - \frac{i}{k_n}\tan\Lambda(\bar{\gamma}_{i,\bar{y}}\ \bar{\gamma}_{j,\bar{x}})\Big]A_{ah}$$

$$+ \bar{y}_{i,\bar{x}}\ \bar{y}_{j,\bar{x}} A_{a\alpha} + b \tan \Lambda(\bar{y}_{i,\overline{xy}}\ \bar{y}_{j,\bar{x}}) A_{a\tau}\}\ d\bar{y} \qquad [3.2.7]$$

The integral equations for the aerodynamic matrix are obtained by substituting the expressions for the aerodynamic coefficients, and the displacement functions $\bar{y}$'s into the expression for the virtual work of the non-conservative forces. The integration is performed numerically by a 15 point gaussian quadrature numerical integration scheme [23]. The roots of the Legendre Polynomial and the weight factors used in the numerical integration are given in Table 1.

Table 1: Abscissas and Weights in Gaussian Quadrature, n = 15

Abscissas	Weights
0.000000000000000	0.202578241925561
+/-0.201194093997435	0.198431485327111
+/-0.394151347077563	0.186161000115562
+/-0.570972172608539	0.166269205816994
+/-0.724417731360170	0.139570677926154
+/-0.848206583410427	0.107159220467172
+/-0.937273392400706	0.070366047488108
+/-0.987992518020485	0.030753241996117

3.3 *Flutter Analysis*

The V-g method [24] was used in computing the flutter speeds. This method introduces a structural damping coefficient g into the equations of motion. Neutral stability (flutter) is attained for a given velocity, when the damping of the structure goes to zero. Assuming harmonic motion the equations of motion become:

$$[[K](1 + ig) - \omega^2[M]]\{C\} = \omega^2[A]\{C\} \qquad [3.3.1]$$

In the absence of non-aerodynamic forces, the resulting generalized eigenvalue problem can be written as:

$$[[I]\lambda - [B]]\{C_i\} = \{0\} \qquad [3.3.2]$$

B is a generalized complex matrix, λ is the eigenvalue and $\{C\}$ is the eigenvector. The eigenvalue λ is defined as:

$$\lambda = \frac{1 + ig}{\omega^2} \qquad [3.3.3]$$

The generalized complex bar matrix bar [B] is defined as:

$$[B] = [K]^{-1}[M + A] \qquad [3.3.4]$$

The flutter speed perpendicular to the midchord is defined as:

$$V_n = \frac{\omega b}{k_n}\cos\Lambda \qquad [3.3.5]$$

Where b is defined as the halfchord perpendicular to the midchord reference line. The flutter frequency bar is ω, and k_n is the reduced frequency.

4.0 Validation of Analysis Program

4.1 Introduction

This chapter gives comparisons between results found in literature and the present code. The validation process is broken down into four sections. To validate the stiffness matrix, the static deflections are checked. The mass matrix is verified by comparing the natural frequencies of vibration with isotropic as well as composite materials. Once sufficient verification of the structural model is complete, the static aerodynamic loads are checked for divergence of swept and unswept wings. The dynamic aerodynamic matrix is verified by comparing the flutter frequencies and speeds with results found by Castel and Kapania [21] who developed a simple element for the aeroelastic analysis of laminated wings. Their formulation allows for unsymmetric laminations, arbitrary geometry including chord and thickness taper, and multiple sweep angles.

The comparisons made in this presentation are for a wing consisting of top and bottom flat laminated skins rigidly connected as shown in Figure 3. For all isotropic comparisons, the material properties of the rectangular box beam were taken to be Aluminium:

$$E_{11} = E_{22} = 6.8948 \times 10^{10} \frac{N}{m^2} \qquad \nu_{12} = 0.30$$

The material properties of the material used in the laminated wing are:

$$E_{11} = 6.9 \times 10^{10} \frac{N}{m^2}, \qquad E_{22} = 5.0 \times 10^{10} \frac{N}{m^2} \qquad \nu_{12} = 0.28$$

$$G_{12} = 1.5 \times 10^{10} \frac{N}{m^2} \qquad \rho_{mat} = 2.71 \times 10^{3} \frac{kg}{m^3}$$

It should be noted that the material properties were arbitrarily chosen.

4.2 *Static Deflections*

The static deflections are compared with Beer and Johnston [22], and Castel and Kapania [21]. For tip loading of a uniform cantilever beam, Beer and Johnston [22] give the tip deflection to be:

$$Z = -\frac{Pl^3}{3EI} \qquad (positive\ up) \qquad [4.2.1]$$

Comparisons with the results obtained using the EPFAC (Equivalent Plate Flutter Analysis Code) are given in Table 2, for different aspect ratios, AR.

Next, the tip deflection under the same loading condition was tested against results of Castel and Kapania [22] for the wing in Figure 3. In this formulation, Castel and Kapania used four finite elements to model the structure. Each beam element has twenty-four degrees of freedom, twelve at each end. Results for zero sweep and variation in fiber angle are given in Figure 5. Excellent agreement between the finite element code and EPFAC exsists for the entire range of values of the fiber angle.

Figure 6 gives a clear comparison between the two different models. EPFAC is termed a skewed wing while the model of reference 21 is a rotated wing. The differences in deflections obtained using the different modeling of the wing structure can be accounted for as follows. The rotated wing's boundary conditions are such that the analysis procedure assumes an effective root and tip perpendicular to the reference line, regardless of sweep angle. As a result, the static deflections are independent of the sweep. The skewed wing assumes the root and tip parallel to the flow. As the wing is swept forward or backward, the torsional and bending stiffnesses become coupled. Static deflection comparisons for different sweep angles of the composite material are given in Figure 7.

4.3 Free Vibration Analysis

For the wing under consideration, the natural frequencies obtained from the present code EPFAC was compared with those obtained using the expressions for a uniform Bernoulli-Euler Cantilever Beam [25]. The comparisons of these values are shown in Table 3. The results show excellent agreement for different aspect ratios.

EPFAC was compared with Ref. [21], for an unswept wing having different ply angles. The results are plotted in Figure 8. The natural frequencies of forward and aft swept wings were also tested. The results are shown in Figure 9. The differences between the two sets of results at larger sweep angles are due to the differences in modeling of the boundary conditions, in the two studies as discussed previously in section 4.2.

Table 2 : Comparisons of Tip Deflections (meters) for Different Aspect Ratios

AR	EPFAC	Eqn. 4.2.1	%diff
5	- 0.04748	-0.04646	2.14
10	-0.18995	-0.18587	2.15
20	-0.75968	-0.74342	2.14
30	-1.71032	-1.67408	2.12

Table 3: Comparison of Natural Frequencies (rad/sec) for Different Aspect Ratios

AR	Mode	EPFAC	Ref.24
5	1	9.015	9.040
	2	56.349	56.674
	3	157.832	158.732
10	1	4.490	4.522
	2	28.085	28.334
	3	78.627	79.356
20	1	2.242	2.261
	2	14.027	14.169
	3	39.250	39.682

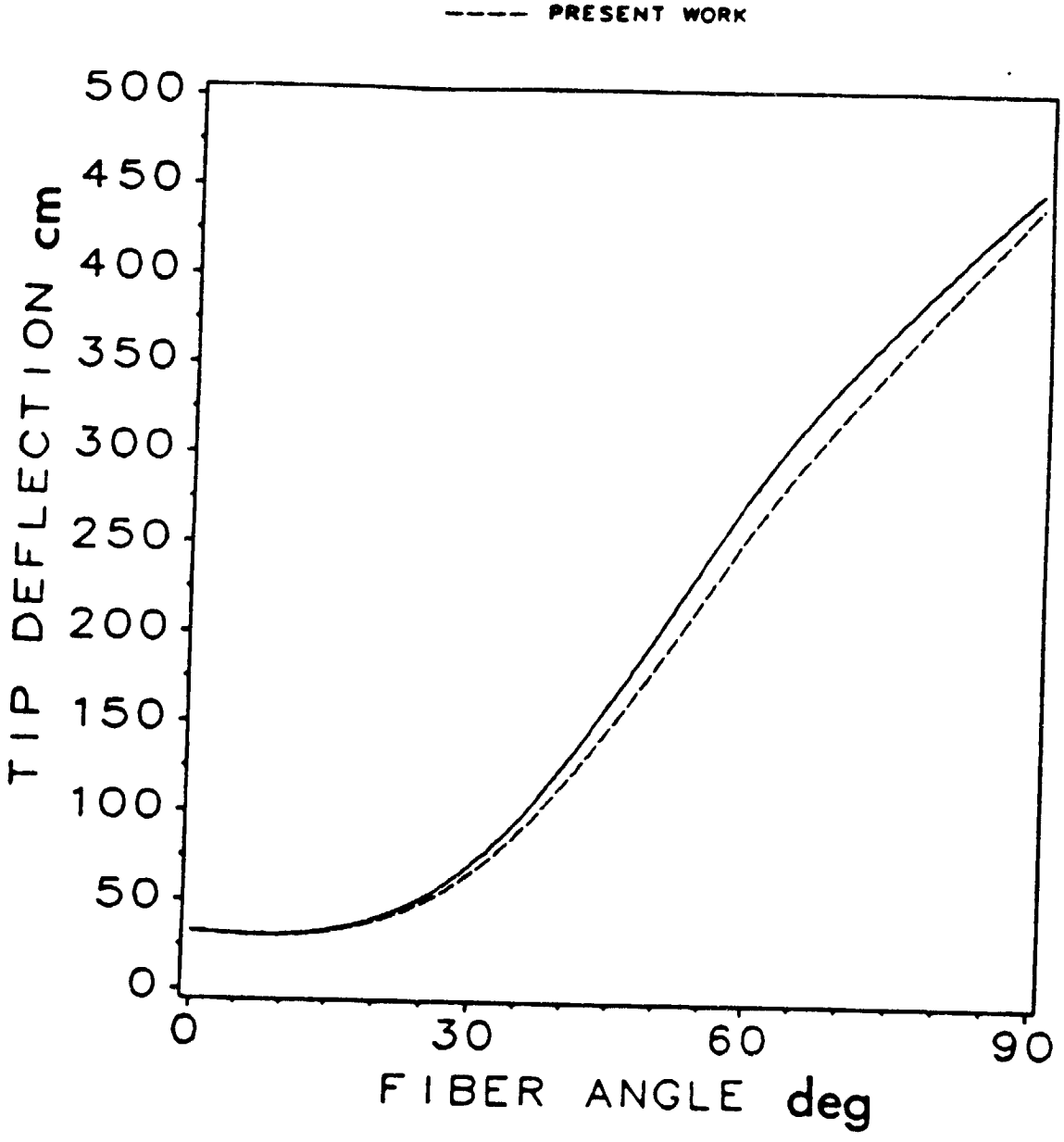

Figure 5 Tip Deflection Comparison of Box Beam at Zero Sweep

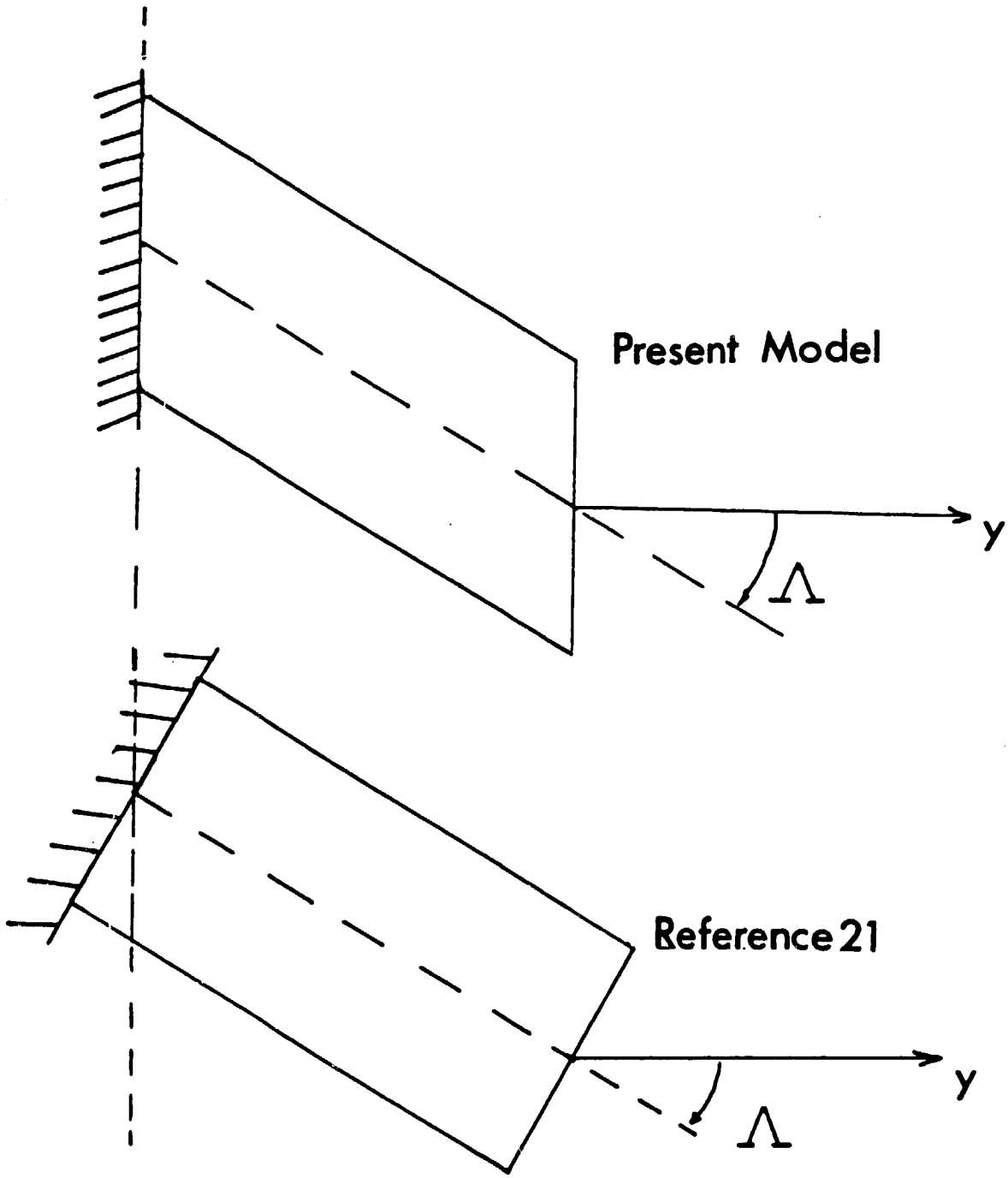

Figure 6 Comparison of Wing Geometries with Ref. [21]

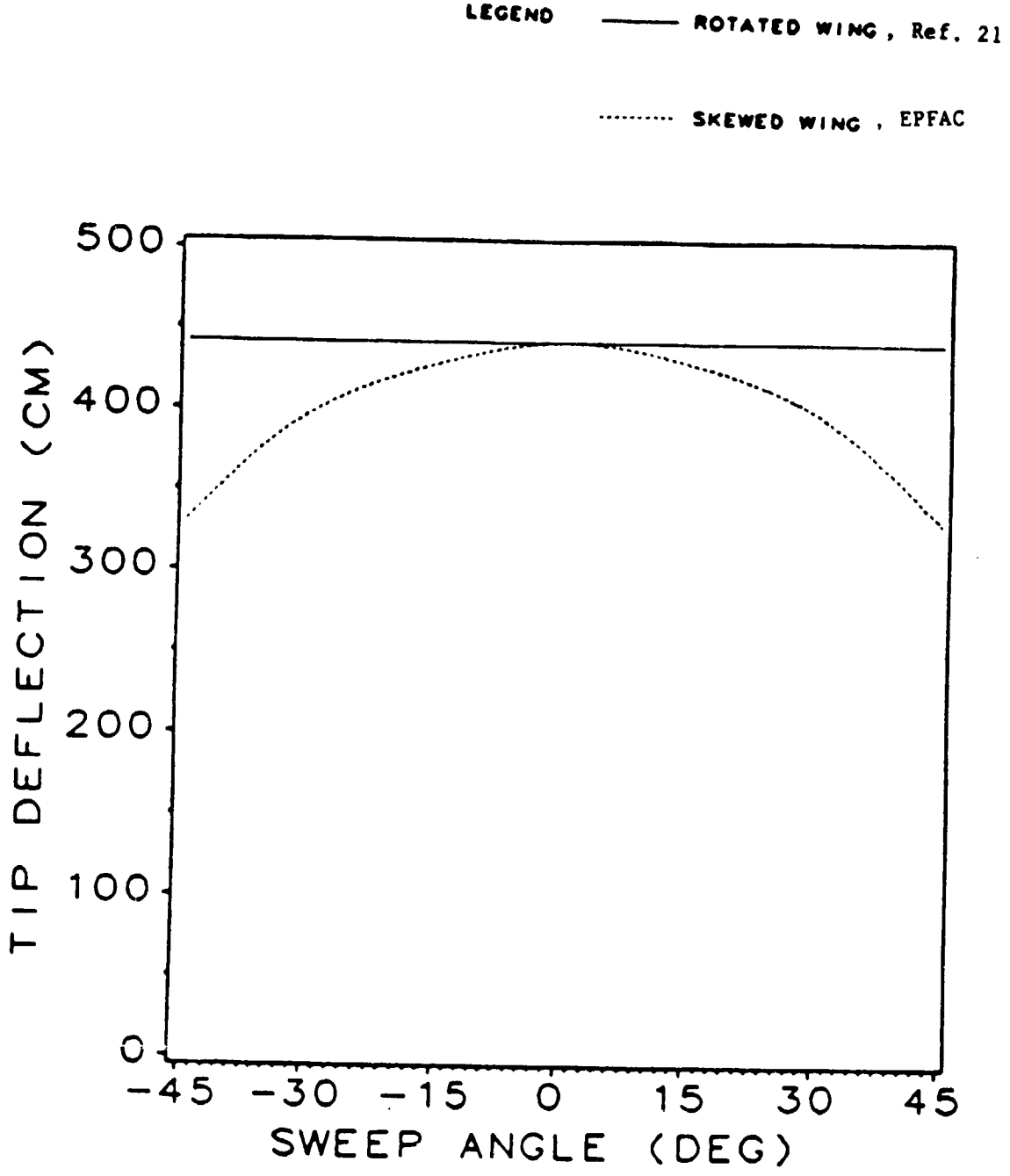

Figure 7 Tip Deflection Comparison for Different Sweep Angles

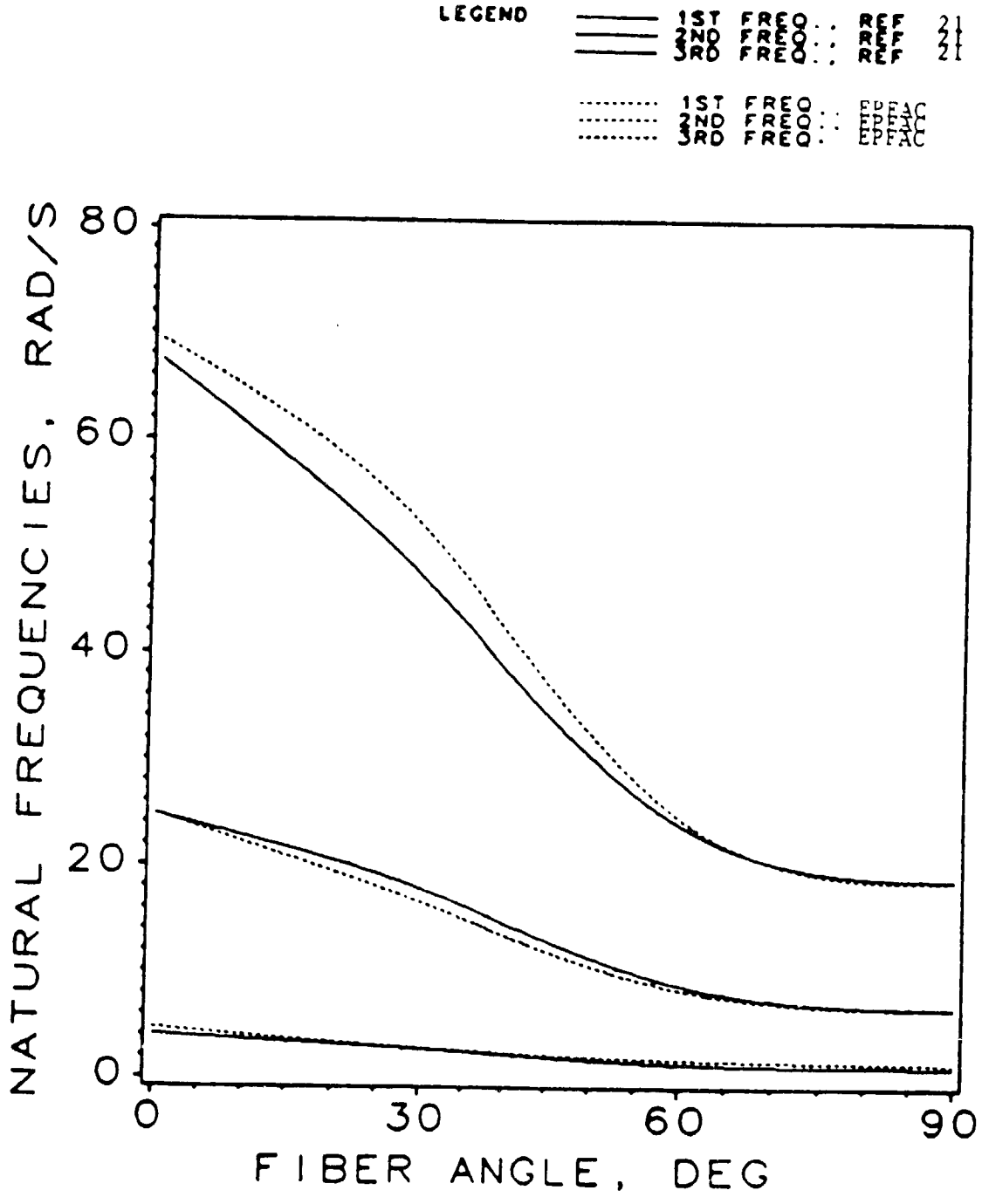

Figure 8 Variation of the Natural Frequencies with Fiber Angle

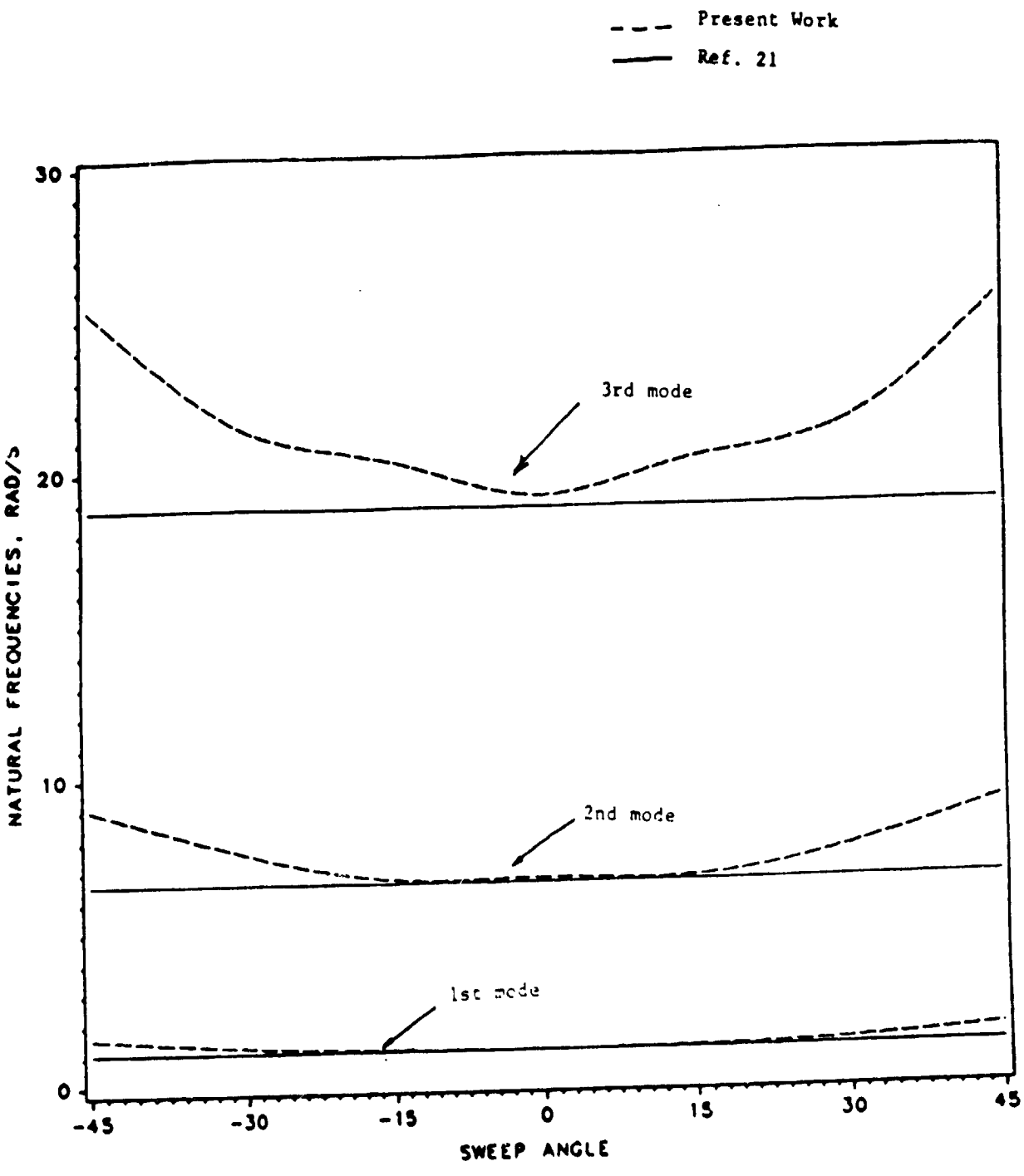

Figure 9 Variation of the Natural Frequencies with Sweep Angle

4.4 *Divergence and Flutter*

Having gained confidence in the structural model, the results for aeroelastic response of swept and unswept wings were compared with the results from two different codes: (i) a code written by Barthelemy and Bergen [17], and (ii) a code written by Castel and Kapania [21]. Barthelemy and Bergen used Weissinger's L-Method to obtain the static aerodynamic loading matrix.

In Weissinger's L-met· od, the flow around the wing is modeled by a lifting line of vortices bound at the wing quarter-chord line. A no-pentration boundary condition is specified at *na* control stations along the win◦ The placement of the control points determines the spanwise distribution of ' . modification to the position of the downwash distribution was employed to account for the slope of the C_l *vs* α curve less than 2π.

The wing dimensions used for comparison with the present method are:

$$S = 20.0\,m^2 \quad AR = 10.0 \qquad tp = 1.0$$

where *tp* is the taper ratio of the half wing. The results are shown in Figure 10. An excellent agreement is observed between the two sets of results.

Castel and Kapania [21] used Yates' modified strip method [3] to obtain both the static and dynamic aerodynamic loadings for swept and unswept composite wings. For different values of sweep the fiber orientation was varied and the results for the divergence and flutter speeds were obtained with EPFAC. Figures 11-15, show the comparison

between the results obtained using the EPFAC code and that of Castel and Kapania for divergence and flutter speeds for different values of sweep and fiber orientation. The differences at large sweep angles are due to the different models used in the two studies. As discussed previously in the section on deflection in this chapter, the model used in Reference [21] is a rotated model, compared to a skewed model used in EPFAC

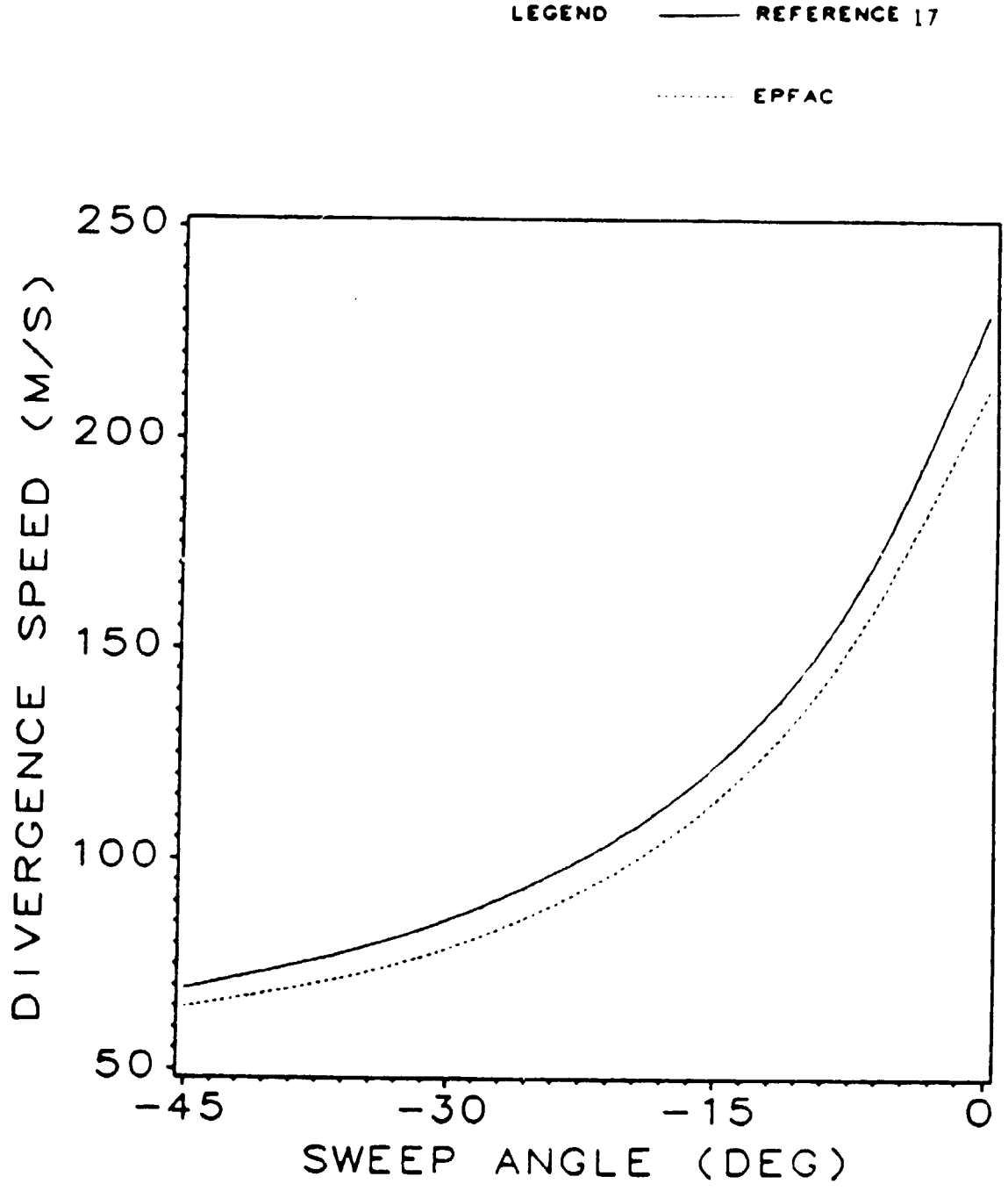

Figure 10 Variation of Divergence Speed with Sweep Angle

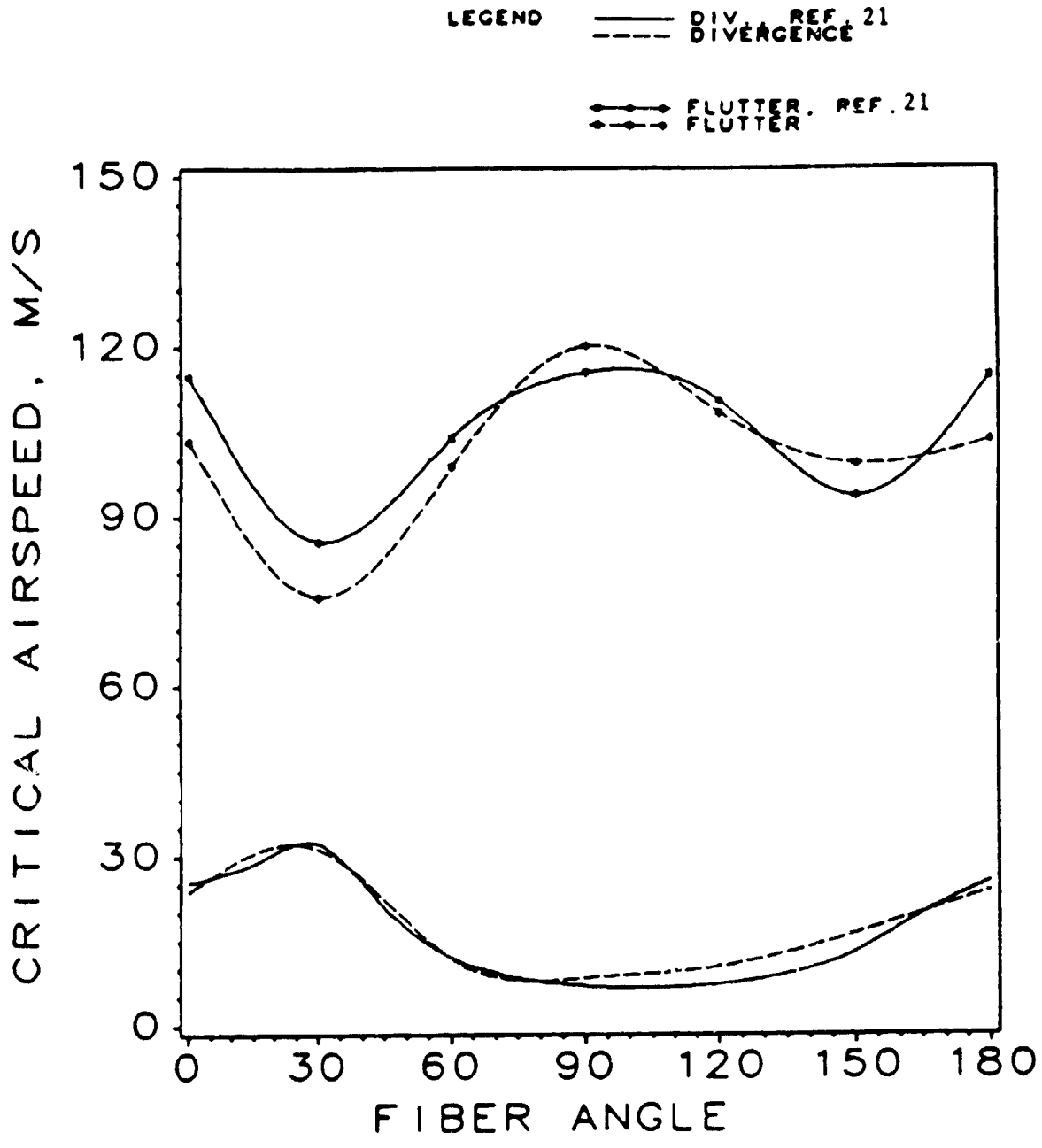

Figure 11 Divergence and Flutter Speeds of a 45 ° Sweptforward Box Beam

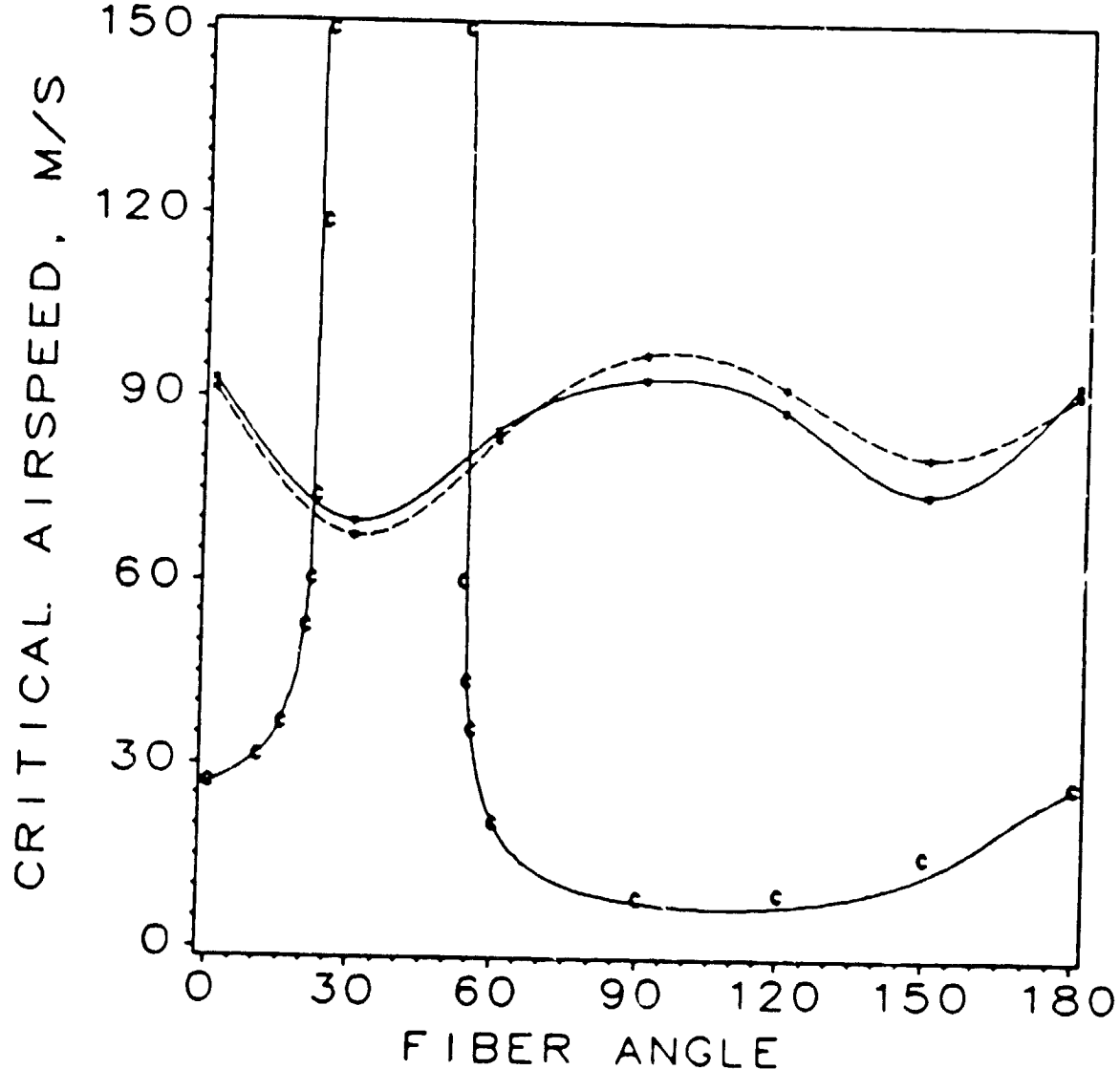

Figure 12 Divergence and Flutter Speeds of a 30 ° Sweptforward Box Beam

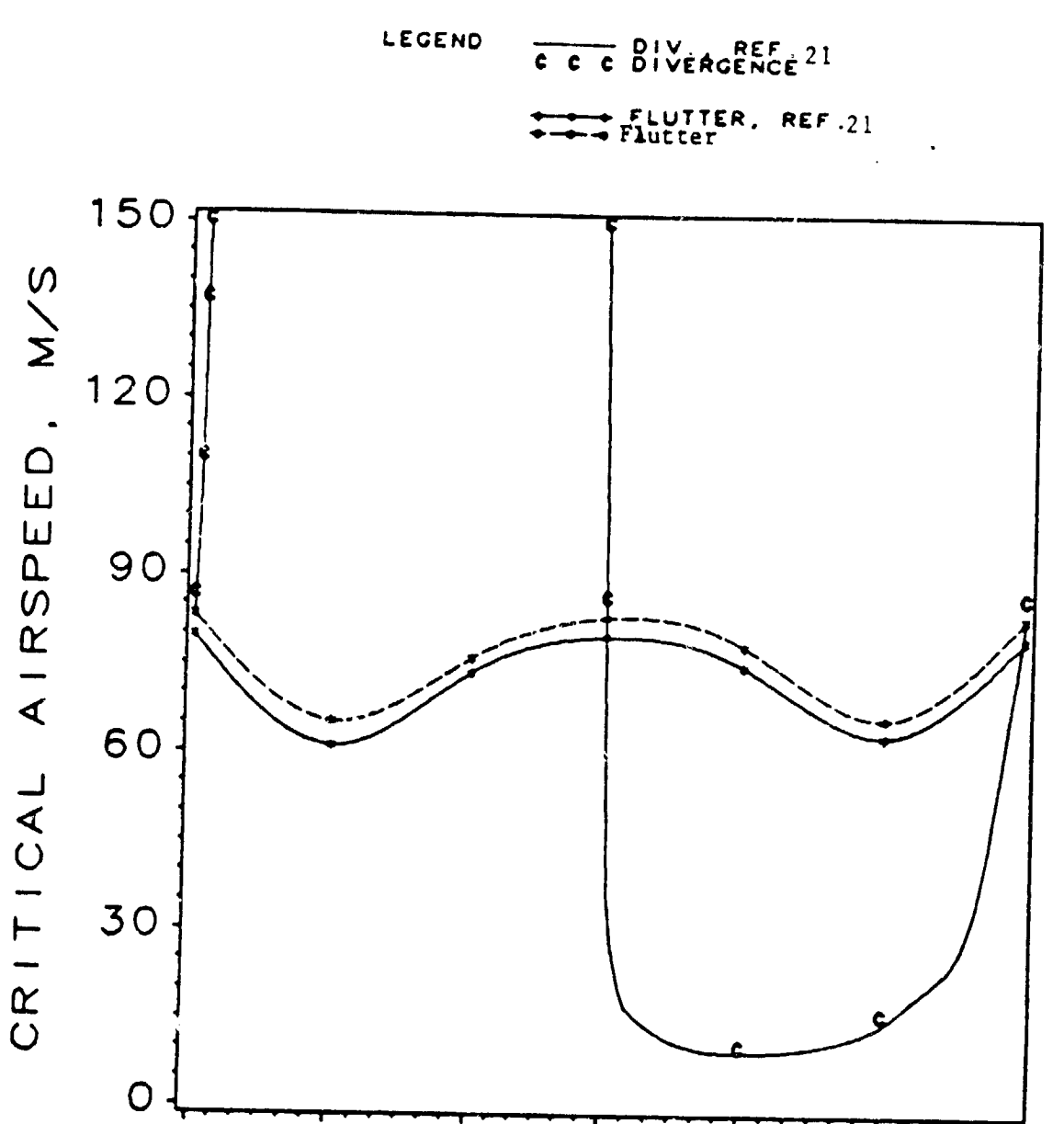

Figure 13 Divergence and Flutter Speeds of a Unswept Box Beam

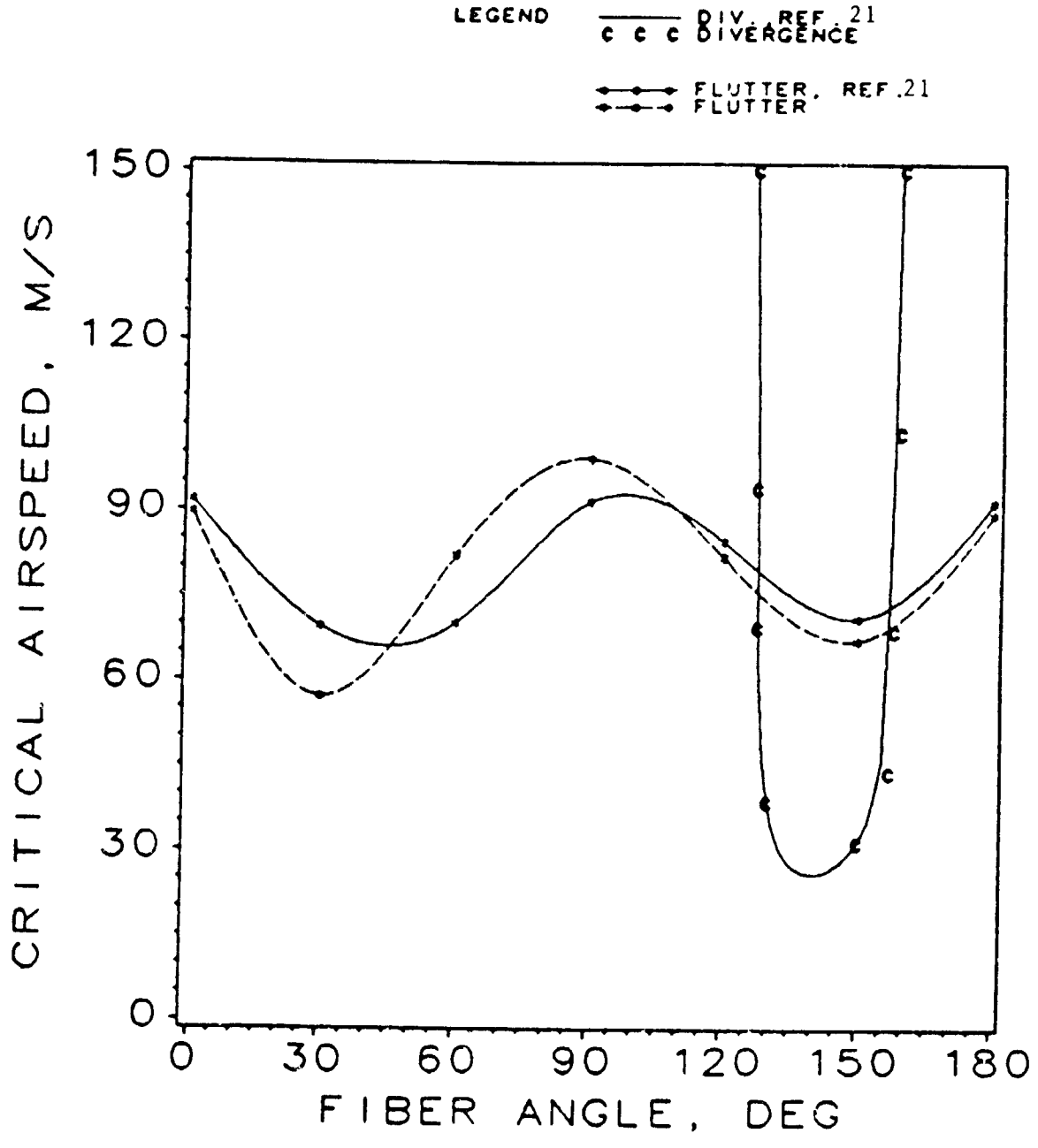

Figure 14 Divergence and Flutter Speeds of a 30 ° Sweptback Box Beam

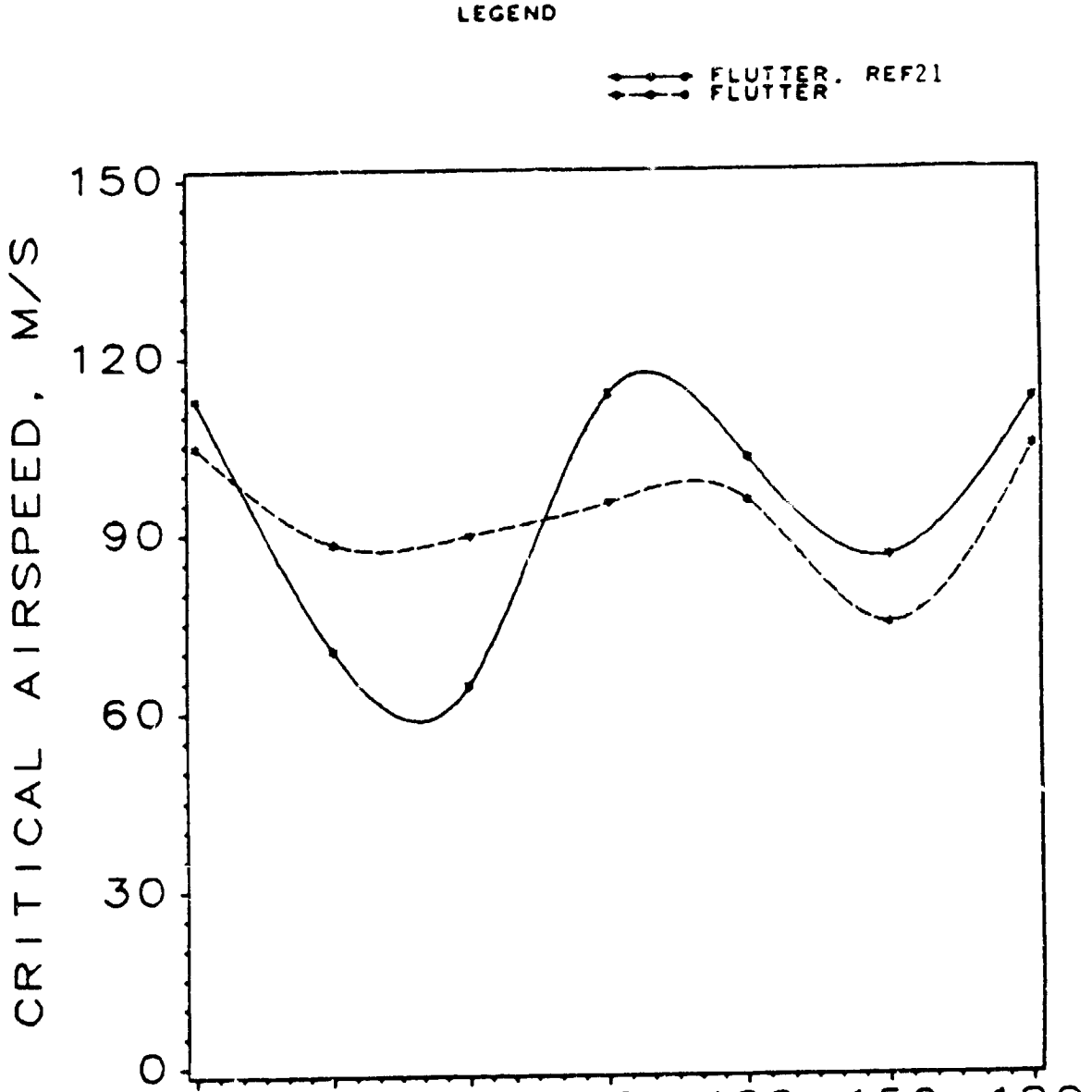

Figure 15 Flutter Speeds of a 45 ° Sweptback Box Beam

5.0 Sensitivity Analysis

5.1 Introduction

This chapter presents the calculation for the sensitivity of the flutter speed, flutter frequency, and reduced frequency to geometric shape parameters namely: (i) aspect ratio, (ii) surface area, (iii) taper ratio, and (iv) sweep angle. The sensitivity calculations require the sensitivity of the aerodynamic, mass and stiffness matrices with respect to various shape parameters. A key objective of this study is to check the viability of calculating the desired derivatives using an analytical approach. It was decided to analytically obtain the sensitivities of the aerodynamic matrix. The analytical derivatives eliminate the uncertainty in the choice of step size which if too large can can lead to truncation errors and if too small can lead to ill-conditioning.

The derivation of the analytic derivative of the aerodynamic matrix, is given in this chapter. To validate the expressions for the eigenvalue derivatives, these derivatives are calculated using three different methods. The first method is purely a numerical ap-

proach that uses a finite difference approximation to find the eigenvalue derivatives. The second method is a semi-analytic approach, because the derivatives of the aerodynamic matrix are found using finite difference approximations, and then using the expression for the derivative of the eigenvalue as given by Murthy and Haftka [19]. The third "analytic" method uses an analytically derived derivative of the aerodynamic matrix, along with the eigenvalue derivative expression given by Murthy and Haftka [19].

5.2 *Eigenvalue Derivatives and Solution Procedures*

In the first method of calculating the derivatives, the flutter problem is solved twice and the derivatives of the eigenvalues are approximated using a forward finite difference scheme.

The second and third methods use the expression for the eigenvalue derivative as given by Murthy and Haftka [19]. The expression is derived using the main and the adjoint problem. The main eigenvalue problem is:

$$[[\Gamma]\lambda - [B]]\{e_r\} = \{0\} \qquad [5.2.1]$$

where e_r is the right hand eigenvector, and [B] is defined in equation 3.3.4. Similiarly the adjoint problem is:

$$\{e_l\}^t[[\Gamma]\lambda - [B]] = \{0\}^t \qquad [5.2.2]$$

where e_l is the left hand eigenvector. The eigenvalues in both cases are the same. Taking the derivative of equation 5.2.1 with respect to a shape parameter p_s yields:

$$[[I]\frac{\partial \lambda}{\partial p_s} - \frac{\partial [B]}{\partial p_s}]\{e_r\} + [[I]\lambda - [B]]\{\frac{\partial e_r}{\partial p_s}\} = 0 \qquad [5.2.3]$$

Multiplying the above equation by left eigenvector gives:

$$\{e_l\}^t [[I]\frac{\partial \lambda}{\partial p_s} - \frac{\partial [B]}{\partial p_s}]\{e_r\} + \{e_l\}^t [[I]\lambda - [B]]\{\frac{\partial e_r}{\partial p_s}\} = 0 \qquad [5.2.4]$$

Equation 5.2.2 reduces this to:

$$\{e_l\}^t [[I]\frac{\partial \lambda}{\partial p_s} - \frac{\partial [B]}{\partial p_s}]\{e_r\} = 0 \qquad [5.2.5]$$

For the i^{th} eigenvalue, the eigenvalue derivative is expressed as:

$$\frac{\partial \lambda^i}{\partial p_s} = \frac{\{e_l^i\}^t \frac{\partial [B]}{\partial p_s}\{e_r^i\}}{\{e_l^i\}^t\{e_r^i\}} \qquad [5.2.6]$$

Recalling equation 3.3.3, the eigenvalue derivative in terms of flutter frequency, damping, and there derivatives is written as:

$$\frac{\partial \lambda}{\partial p_s} = -\frac{2\frac{\partial \omega}{\partial p_s}}{\omega^3} + \frac{[\frac{\partial g}{\partial p_s}\omega^2 - 2\omega\frac{\partial \omega}{\partial p_s}g]}{\omega^4} i \qquad [5.2.7]$$

To obtain the derivative of the generalized complex matrix [B], the derivatives of the aerodynamic matrix [A]; of the inverse of the stiffness matrix $[K]^{-1}$, and of the mass matrix [M] are needed.

$$\frac{d[B]}{dp_s} = \frac{\partial[K]^{-1}}{\partial p_s}[[M] + [A]] + [K]^{-1}\left[\frac{\partial[M]}{\partial p_s} + \frac{d[A]}{dp_s}\right] \qquad [5.2.8]$$

The derivatives of the mass matrix, and the inverse of the stiffness matrix are obtained using the forward finite difference method. A study was first conducted to obtain an appropriate step size for the finite difference calculations. The results of this study are shown in Table 4. These step sizes indicate that the calculated derivatives are stable as indicated in Table 4.

The derivatives of the aerodynamic matrix [A] with respect to a geometric shape parameter are obtained using two different methods: (i) finite difference method; and (ii) analytic method. The calculation of the sensitivity of the aerodynamic matrix [A] is made difficult by the fact that this matrix depends upon shape parameters p_s and also on the reduced frequency k_n. The reduced frequency is not really an independent variable, as its value for a new value of $p_s (= p_s^{old} + \Delta p_s)$ should be such that the imaginary part of the eigenvalue corresponding to the perturbed configuration should be zero.

In the finite difference method, the sensitivity of the aerodynamic matrix [A] is obtained as follows:

$$\frac{d[A]}{dp_s} = \frac{[A(p_s + \Delta p_s, k_n + \Delta k_n)] - [A(p_s, k_n)]}{\Delta p_s} \qquad [5.2.9]$$

To obtain the value of Δk_n, an iterative procedure, as described in Figure 16, is used. As a first step, Δk_n is put equal to zero, and the sensitivity of the eigenvalue is obtained. Obviously, the imaginary part of the new eigenvalue thus obtained will not be zero. This fact is used to obtain the value of Δk_n as explained in the following.

The change in the damping coefficient g, a function of both the shape parameters and reduced frequency, can be written as:

$$dg = \frac{\partial g}{\partial p_s}\, dp_s + \frac{\partial g}{\partial k_n}\, dk_n \qquad [5.2.10]$$

At flutter speed:

$$g = 0 \quad , \quad dg = 0$$

Therefore

$$\frac{dk_n}{dp_s} = -\frac{\dfrac{\partial g}{\partial p_s}}{\dfrac{\partial g}{\partial k_n}} \qquad [5.2.11]$$

Note that $\frac{\partial g}{\partial k_n}$ was already obtained during the calculations of the flutter speed. The values of reduced frequency are varied in the intial problem to compute the value at the point the damping coefficient goes to zero. Therefore, $\frac{\partial g}{\partial k_n}$ is easily computed by a forward finite difference scheme. The value of $\frac{\partial g}{\partial p_s}$ is obtained from the imaginary part of the sensitivity of the eigenvalue obtained in the first step. This is computed directly from the eigenvalue derivative. Recalling equation 5.2.7:

$$\frac{\partial g}{\partial p_s} = imag\left(\frac{\partial \lambda}{\partial p_s}\right)\ \omega^2 + \frac{2\frac{\partial \omega}{\partial p_s} g}{\omega} \qquad [5.2.12]$$

where ω is obtained from the orginal flutter problem and;

$$\frac{\partial \omega}{\partial p_s} = -\frac{real\left(\frac{\partial \lambda}{\partial p_s}\right)\ \omega^3}{2} \qquad [5.2.13]$$

If $\frac{\partial g}{\partial p_s}$ is not within a tolerance of 10^{-6}, the aerodynamic matrix [A] is recalculated at a new value of the reduced frequency while also keeping the same perturbation in the shape parameter. Once $\frac{dk_n}{dp_s}$ is known, an approximation to the value of k_n, corresponding to flutter speed for a new value of p_s, is obtained using a Taylor's series expansion:

$$k_n^{new} = k_n^{old} + \frac{dk_n}{dp_s}\ \Delta p_s \qquad [5.2.14]$$

This process is repeated until the tolerance is met.

In the "analytical" method, the sensitivity of the generalized complex matrix [B] is obtained in a similiar fashion except the sensitivity of the aerodynamic matrix [A] is computed analytically. This is expressed as follows:

$$\frac{d[A]}{dp_s} = \frac{\partial [A]}{\partial p_s} + \frac{\partial [A]}{\partial k_n}\ \frac{dk_n}{dp_s} \qquad [5.2.15]$$

Both $\frac{\partial [A]}{\partial p_s}$ and $\frac{\partial [A]}{\partial k_n}$ are derived in section 5.4. The value of $\frac{dk_n}{dp_s}$ is computed from the eigenvalue derivative, as explained above. In the first iteration, $\frac{dk_n}{dp_s}$ is assumed to be zero. The aerodynamic matrix derivative is computed and combined with the deriva-

tives of the mass [M], inverse stiffness matrices $[K]^{-1}$ to form $\frac{\partial [B]}{\partial p_s}$. The eigenvalue derivative is then computed. The value of $\frac{dk_n}{dp_s}$ is calculated as described above. Figure 17 shows a detailed flow chart of the analytic method.

The derivative of the flutter speed is:

$$\frac{\partial V_f}{\partial p_s} = \frac{[k_n[\ \frac{\partial \omega}{\partial p_s} b + \omega \frac{\partial b}{\partial p_s}\ ] - \omega b \frac{\partial k_n}{\partial p_s}\ ]}{k_n^2} \qquad [5.2.16]$$

The flutter speed at the new configuration is then computed using a truncated taylor series. As before:

$$V_f^{new} = V_f^{old} + \frac{\partial V_f}{\partial p_s} \Delta p_s \qquad [5.2.17]$$

To calculate the analytic derivative of the aerodynamic matrix, the geometric parameters must first be defined.

5.3 *Geometric Parameters*

The Aerodynamic matrix is composed of geometric parameters which are a function of surface area, aspect ratio, taper ratio and sweep angle. These parameters are the span, root chord, tip chord, halfchord, the global x and y coordinates, the displacement functions, and their derivatives with respect to global x and y coordinates. These are expressed as:

$$B = \sqrt{AR\,S} \qquad [5.3.1]$$

$$C_r = \frac{2S}{(1+tp)\sqrt{AR\,S}} \qquad [5.3.2]$$

$$C_t = \frac{2S\,tp}{(1+tp)\sqrt{AR\,S}} \qquad [5.3.3]$$

$$crd(i) = C_r + (C_t - C_r)\frac{(\eta(i)+1)}{2} \qquad i = 1,\ldots,15 \qquad [5.3.4]$$

$$x(i) = \frac{C_r}{2} + y(i)\tan\Lambda \qquad i = 1,\ldots,15 \qquad [5.3.5]$$

$$y(i) = \frac{B\eta(i) + B}{2} \qquad i = 1,\ldots,15 \qquad [5.3.6]$$

$$b(i) = \frac{crd(i)}{2}\cos\Lambda \qquad i = 1,\ldots,15 \qquad [5.3.7]$$

Where b is the halfchord measured perpendicular to the reference line , AR is the aspect ratio, S is the surface area, C_r is the root chord, C_t is the tip chord, crd(i) is the chord length at station i , and tp is the taper ratio.

5.4 *Analytic Derivatives*

For general purposes, p_s will represent the shape parameters, where s = 1 is the surface area, s = 2 is the aspect ratio, s = 3 is the taper ratio, and s = 4 is the sweep angle. The

Aerodynamic matrix, given in equation 3.2.7, must be differentiated with respect to the shape parameters and the reduced frequency. In order to avoid the use of Lebnitz's Rule, and facilitating numerical integration using Gauss integration, the intergrals must be changed over to local coordinates. Equation 3.2.7 is written as:

$$A_{ji} = -\int_{-1}^{1} \pi\rho b^3\omega^2 \; [[\frac{1}{b}(\bar{\gamma}_i\ \bar{\gamma}_j) - \frac{i}{k_n}\tan\Lambda(\bar{\gamma}_{i,\bar{y}}\ \bar{\gamma}_j)]A_{ch}$$

$$+ \bar{\gamma}_{i,\bar{x}}\ \bar{\gamma}_j A_{c\alpha} + b\tan\Lambda(\bar{\gamma}_{i,\overline{xy}}\ \bar{\gamma}_j)A_{c\tau}]\frac{B}{2\cos\Lambda}\quad d\eta$$

$$-\int_{-1}^{1} \pi\rho b^4\omega^2[[\frac{1}{b}(\bar{\gamma}_i\ \bar{\gamma}_{j,\bar{x}}) - \frac{i}{k_n}\tan\Lambda(\bar{\gamma}_{i,\bar{y}}\ \bar{\gamma}_{j,\bar{x}})]A_{ah} \qquad [5.4.1]$$

$$+ \bar{\gamma}_{i,\bar{x}}\ \bar{\gamma}_{j,\bar{x}}A_{a\alpha} + b\tan\Lambda(\bar{\gamma}_{i,\overline{xy}}\ \bar{\gamma}_{j,x})A_{a\tau}]\ \frac{B}{2\cos\Lambda}\quad d\eta$$

where $d\bar{y}$ is replaced by $\frac{B}{2\cos\Lambda}d\eta$.

The derivative of the aerodynamic matrix with respect to a general shape parameter, representing $B' = \frac{B}{\cos\Lambda}$, is:

$$\frac{dA_{ji}}{dp_s} = -\pi\rho\omega^2[\int_{-1}^{1}[(2b\frac{\partial b}{\partial p_s}\bar{\gamma}_i\bar{\gamma}_j + b^2\frac{\partial\bar{\gamma}_i}{\partial p_s}\bar{\gamma}_j + b^2\bar{\gamma}_i\frac{\partial\bar{\gamma}_j}{\partial p_s}\}\ A_{ch}$$

$$-[\frac{3ib^2}{k_n}\frac{\partial b}{\partial p_s}\bar{\gamma}_{i,\bar{y}}\bar{\gamma}_j\tan\Lambda + \frac{ib^3}{k_n}\frac{\partial\bar{\gamma}_{i,\bar{y}}}{\partial p_s}\bar{\gamma}_j\tan\Lambda + \frac{ib^3}{k_n}\bar{\gamma}_{i,\bar{y}}\frac{\partial\bar{\gamma}_j}{\partial p_s}\tan\Lambda$$

$$+\frac{ib^3}{k_n\cos^2\Lambda}\bar{\gamma}_{i,\bar{y}}\bar{\gamma}_j\frac{\partial\Lambda}{\partial p_s} - \frac{ib^3}{k_n^2}\bar{\gamma}_{i,\bar{y}}\bar{\gamma}_j\tan\Lambda\frac{\partial k_n}{\partial p_s}]\ A_{ch}$$

$$+ (3b^2 \frac{\partial b}{\partial p_s} \bar{\gamma}_{i,\bar{x}} \bar{\gamma}_j + b^3 \frac{\partial \bar{\gamma}_{i,\bar{x}}}{\partial p_s} \bar{\gamma}_j + b^3 \bar{\gamma}_{i,\bar{x}} \frac{\partial \bar{\gamma}_j}{\partial p_s}) \; A_{cx}$$

$$+ (4b^3 \frac{\partial b}{\partial p_s} \bar{\gamma}_{i,\overline{xy}} \bar{\gamma}_j \tan\Lambda + b^4 \frac{\partial \bar{\gamma}_{i,\overline{xy}}}{\partial p_s} \bar{\gamma}_j \tan\Lambda + b^4 \bar{\gamma}_{i,\overline{xy}} \frac{\partial \bar{\gamma}_j}{\partial p_s} \tan\Lambda + \frac{b^4}{\cos^2\Lambda} \bar{\gamma}_{i,\overline{xy}} \bar{\gamma}_j \frac{\partial \Lambda}{\partial p_s}) \; A_{c\tau}$$

$$+ (3b^2 \frac{\partial b}{\partial p_s} \bar{\gamma}_i \bar{\gamma}_{j,\bar{x}} + b^3 \frac{\partial \bar{\gamma}_i}{\partial p_s} \bar{\gamma}_{j,\bar{x}} + b^3 \bar{\gamma}_i \frac{\partial \bar{\gamma}_{j,\bar{x}}}{\partial p_s}) \; A_{ah}$$

$$- [\frac{4ib^3}{k_n} \frac{\partial b}{\partial p_s} \bar{\gamma}_{i,\bar{y}} \bar{\gamma}_{j,\bar{x}} \tan\Lambda + \frac{ib^4}{k_n} \frac{\partial \bar{\gamma}_{i,\bar{y}}}{\partial p_s} \bar{\gamma}_{j,\bar{x}} \tan\Lambda + \frac{ib^4}{k_n} \bar{\gamma}_{i,\bar{y}} \frac{\partial \bar{\gamma}_{j,\bar{x}}}{\partial p_s} \tan\Lambda$$

$$+ \frac{ib^4}{k_n \cos^2\Lambda} \bar{\gamma}_{i,\bar{y}} \bar{\gamma}_{j,\bar{x}} \frac{\partial \Lambda}{\partial p_s} - \frac{ib^4}{k_n^2} \bar{\gamma}_{i,\bar{y}} \bar{\gamma}_{j,\bar{x}} \tan\Lambda \frac{\partial k_n}{\partial p_s}] \; A_{ah}$$

$$+ (4b^3 \frac{\partial b}{\partial p_s} \bar{\gamma}_{i,\bar{x}} \bar{\gamma}_{j,\bar{x}} + b^4 \frac{\partial \bar{\gamma}_{i,\bar{x}}}{\partial p_s} \bar{\gamma}_{j,\bar{x}} + b^4 \bar{\gamma}_{i,\bar{x}} \frac{\partial \bar{\gamma}_{j,\bar{x}}}{\partial p_s}) \; A_{ax}$$

$$+ [5b^4 \frac{\partial b}{\partial p_s} \bar{\gamma}_{i,\overline{xy}} \bar{\gamma}_{j,\bar{x}} \tan\Lambda + b^5 \frac{\partial \bar{\gamma}_{i,\overline{xy}}}{\partial p_s} \bar{\gamma}_{j,\bar{x}} \tan\Lambda + b^5 \bar{\gamma}_{i,\overline{xy}} \frac{\partial \bar{\gamma}_{j,\bar{x}}}{\partial p_s} \tan\Lambda$$

$$+ \frac{b^5}{\cos^2\Lambda} \bar{\gamma}_{i,\overline{xy}} \bar{\gamma}_{j,\bar{x}} \frac{\partial \Lambda}{\partial p_s}] A_{a\tau} \qquad [5.4.2]$$

$$+ [b^2 \bar{\gamma}_i \; \bar{\gamma}_j - \frac{ib^3}{k_n} \tan\Lambda \bar{\gamma}_{i,\bar{y}} \; \bar{\gamma}_j] \frac{\partial A_{ch}}{\partial p_s} + b^3 \bar{\gamma}_{i,\bar{x}} \bar{\gamma}_j \frac{\partial A_{cx}}{\partial p_s}$$

$$+ (b^4 \tan\Lambda \; \bar{\gamma}_{i,\overline{xy}} \; \bar{\gamma}_j) \frac{\partial A_{c\tau}}{\partial p_s} + [b^3 \bar{\gamma}_i \; \bar{\gamma}_{j,\bar{x}} - \frac{ib^4}{k_n} \tan\Lambda \bar{\gamma}_{i,\bar{y}} \; \bar{\gamma}_{j,\bar{x}}] \frac{\partial A_{ah}}{\partial p_s}$$

$$+ b^4 \bar{\gamma}_{i,\bar{x}} \; \bar{\gamma}_{j,\bar{x}} \frac{\partial A_{ax}}{\partial p_s} + b^5 \tan\Lambda \bar{\gamma}_{i,\overline{xy}} \; \bar{\gamma}_{j,\bar{x}} \frac{\partial A_{a\tau}}{\partial p_s}] \frac{B'}{2}$$

$$+ [[b^2\bar{\gamma}_i\ \bar{\gamma}_j - \frac{i}{k_n}\tan\Lambda\bar{\gamma}_{i,\bar{y}}\ \bar{\gamma}_j]A_{ch} + b^3\bar{\gamma}_{i,\bar{x}}\ \bar{\gamma}_j\ A_{cx}$$

$$+ (b^4\tan\Lambda\ \bar{\gamma}_{i,\overline{xy}}\ \bar{\gamma}_j)A_{c\tau} + [b^3\bar{\gamma}_i\ \bar{\gamma}_{j,\bar{x}} - \frac{ib^4}{k_n}\tan\Lambda\bar{\gamma}_{i,\bar{y}}\ \bar{\gamma}_{j,\bar{x}}]\ A_{ah}$$

$$+ b^4\bar{\gamma}_{i,\bar{x}}\ \bar{\gamma}_{j,\bar{x}}A_{a\alpha} + b^5\tan\Lambda\bar{\gamma}_{i,\overline{xy}}\ \bar{\gamma}_{j,\bar{x}}A_{a\tau}]\frac{\partial B'}{2\partial p_s}]d\eta$$

The derivatives of the displacement function with respect to a general shape parameter p_i are given as follows:

$$\frac{\partial}{\partial p_s} = \frac{\partial}{\partial x}\ \frac{\partial x}{\partial p_s} + \frac{\partial}{\partial y}\ \frac{\partial y}{\partial p_s} \qquad [5.4.3]$$

The global coordinates x and y are given in terms of the local coordinates and the geometric shape parameters in equations 5.3.5 and 5.3.6. The derivatives of x and y with respect to various geometric shape parameters are as follows:

$$\frac{\partial y}{\partial AR} = \frac{S(\eta + 1)}{4(\sqrt{AR\,S})} \qquad [5.4.4]$$

$$\frac{\partial y}{\partial S} = \frac{AR(\eta + 1)}{4(\sqrt{AR\,S})} \qquad [5.4.5]$$

$$\frac{\partial y}{\partial tp} = 0.0 \qquad [5.4.6]$$

$$\frac{\partial y}{\partial \Lambda} = 0.0 \qquad [5.4.7]$$

$$\frac{\partial x}{\partial AR} = -\frac{S^2}{2(1+tp)AR\,S^{\frac{3}{2}}} + \frac{\partial y}{\partial AR}\tan\Lambda \qquad [5.4.8]$$

$$\frac{\partial x}{\partial S} = \frac{1}{2(1+tp)\sqrt{AR\,S}} + \frac{\partial y}{\partial AR}\tan\Lambda \qquad [5.4.9]$$

$$\frac{\partial x}{\partial tp} = -\frac{S\sqrt{AR\,S}}{[(1+tp)]^2} \qquad [5.4.10]$$

$$\frac{\partial x}{\partial \Lambda} = \frac{\sqrt{AR\,S}(\eta+1)}{2\cos^2\Lambda} \qquad [5.4.11]$$

The derivatives of the halfchord with respect to the shape parameters are:

$$\frac{\partial b}{\partial S} = \frac{(1+(tp-1)\eta+tp)\cos\Lambda}{4(1+tp)\sqrt{AR\,S}} \qquad [5.4.12]$$

$$\frac{\partial b}{\partial AR} = -\frac{S^2(1+(tp-1)\eta+tp)\cos\Lambda}{4(1+tp)(S\,AR)^{\frac{3}{2}}} \qquad [5.4.13]$$

$$\frac{\partial b}{\partial tp} = \frac{S\,\eta\ \cos\Lambda}{(1+tp)^2\sqrt{AR\,S}} \qquad [5.4.14]$$

$$\frac{\partial b}{\partial \Lambda} = -\frac{S(1+(tp-1)\eta+tp)\sin\Lambda}{2(1+tp)\sqrt{S\,AR}} \qquad [5.4.15]$$

The aerodynamic coefficients, A_{ch}, A_{ah}, A_{cr}, A_{ah}, A_{ah} and A_{ar}, are functions of the reduced frequency. The reduced frequency changes as the shape parameters change therefore these terms are functions of the shape parameters and must be included in the formulation. They are defined as:

$$\frac{\partial}{\partial p_s} = \frac{\partial}{\partial k_n}\frac{dk_n}{dp_s} \qquad [5.4.16]$$

$$\frac{\partial A_{ch}}{\partial k_n} = \left(\frac{iC_{l\alpha}}{\pi}\right)\frac{k_n\dfrac{dC(k_n)}{dk_n} - C(k_n)}{k_n^2} \qquad [5.4.17]$$

$$\frac{\partial A_{c\alpha}}{\partial k_n} = -\frac{i}{k_n^2} + \left(\frac{iC_{l\alpha}}{\pi}\right)\frac{k_n\dfrac{dC(k_n)}{dk_n} - C(k_n)}{k_n^2}\left(\frac{1}{2} - a\right)$$

$$\left(\frac{C_{l\alpha}}{\pi}\right)\frac{k_n\dfrac{dC(k_n)}{dk_n} - 2C(k_n)}{k_n^3} \qquad [5.4.18]$$

$$\frac{\partial A_{c\tau}}{\partial k_n} = -\frac{ia}{k_n^2} + \frac{k_n\dfrac{dC(k_n)}{dk_n} - C(k_n)}{k_n^2}\left(\frac{C_{l\alpha}}{\pi}\left(-a_{cn} - a\right)\right) \qquad [5.4.19]$$

$$\frac{\partial A_{ah}}{\partial k_n} = -\left(\frac{k_n\dfrac{dC(k_n)}{dk_n} - C(k_n)}{k_n^2}\right)\left(\frac{iC_{l\alpha}}{\pi}\right)\left(-a_{cn} + a\right) \qquad [5.4.20]$$

$$\frac{\partial A_{a\alpha}}{\partial k_n} = -\frac{i}{k_n^2}\left(\frac{1}{2} - a\right) + \left(\frac{k_n\dfrac{dC(k_n)}{dk_n} - 2C(k_n)}{k_n^3}\right)\frac{C_{l\alpha}}{\pi}\left(-a_{cn} + a\right)$$

$$+\left(\frac{k_n\dfrac{dC(k_n)}{dk_n} - C(k_n)}{k_n^2}\right)\left(\frac{iC_{l\alpha}}{\pi}\right)\left(-a_{cn}^2 + a^2\right) \qquad [5.4.21]$$

$$\frac{\partial A_{a\tau}}{\partial k_n} = -\frac{i}{k_n}\left[-\frac{2i}{4k_n^2} + \{-a_{cn}^2 + a^2\}\left(\frac{k_n\frac{dC(k_n)}{dk_n} - C(k_n)}{k_n^2}\right)\left(\frac{C_{l_\alpha}}{\pi}\right)\right] - \frac{1}{k_n}A_{a\tau} \quad [5.4.22]$$

The derivative of Theodorsen's circulation function, as given in equation (3.1.3), is:

$$\frac{dC(k_n)}{dk_n} = \frac{\frac{.0075075i}{k_n^2}}{[1 - \frac{.0455i}{k_n}]^2} + \frac{\frac{.1005i}{k_n^2}}{[1 - \frac{.3i}{k_n}]^2} \quad [5.4.23]$$

The "analytic" derivative of the eigenvalue with respect to various parameters, namely the surface area S, the aspect ratio AR, the taper ratio *tp* and sweep were compared with those obtained using the two previously described methods, namely: (i) the purely finite difference method and (ii) a semi-analytic approach in which the desired derivatives were obtained using a forward finite difference scheme. The results are shown in Table 5. An excellent agreement exists between the various sets of results. However, the values of the derivative of the eigenvalue, with respect to sweep, see fourth row of Table 4, obtained using the three methods appear to be different from each other. For example, the "analytically obtained " derivative (case (iii)) is about 6.95 percent more than that obtained using a purely finite difference approach (case (i)). Similiarly, the value of the same derivative obtained using a semi-analytic approach (case (ii)), is about 9.36 percent less than that obtained using the analytic approach. The reasons for this descrepencies are not entirely clear at this stage. However, Figure 28 shows that the analytic method gives the best results.

Figures 18 through 29 show the flutter speed, frequency, and reduced frequency analytically based values versus the values which where reanalyzed at different configurations.

These are called reanalysis values because the v-g method was used to solve for the flutter speed at the perturbed value. These show excellent agreement over a range which can be useful to the designer in the intial design phase.

However, close attention should be paid to any mode shifting. For instance, in smaller aspect ratio configurations the flutter frequency predominant mode changes from the third mode to the second mode. This evident in Figure 21, where the flutter frequency drops for the lower values of the aspect ratio.

Table 4: Comparison of Finite Difference Step Sizes

ΔS						
1.0	18.934 [a]	50.785 [a]	60.748 [a]	0.9612 [b]	0.2149 [b]	0.0808 [b]
.10	18.945	49.120	57.449	0.9193	0.1987	0.0730
.01 [c]	18.950	48.930	57.100	0.9147	0.1970	0.0723
.001	19.00	48.200	56.100	0.9000	0.1935	0.0709
ΔAR						
1.0	0.0	80.850	119.85	1.7345	0.4812	0.1986
.10	0.0	78.558	109.84	1.6370	0.4153	0.1613
.01 [c]	0.0	78.310	108.83	1.6268	0.4091	0.1579
.001	0.0	78.70	109.30	1.6350	0.4105	0.1583
Δip						
.10	0.0	123.63	122.64	2.1397	0.3583	0.1131
.01	0.0	118.03	117.10	2.0429	0.3421	0.1080
.001 [c]	0.0	117.50	116.60	2.034	0.3406	0.1075
.0001	0.0	116.0	115.00	2.010	0.3370	0.1070
$\Delta\Lambda$						
1.0	61.993	53.302	108.49	.15123	.2566	.04798
.10 [c]	61.811	51.543	108.17	.15079	.2479	.04785
.01	61.765	51.394	108.12	.15075	.2471	.04784
.001	61.307	51.566	107.72	.15069	.2469	.04755

a) These columns represent the finite difference derivatives of the stiffness matrix.

b) These columns represent the finite difference derivatives of the mass matrix.

c) Step size used for finite difference calculations

Table 5: Comparison of Eigenvalue Derivatives w.r.t Four Parameters

	case (i) Finite Difference	case (ii) Semi-Analytic	case (iii) Analytic
S	2.4151 E-5	2.4593 E-5	2.4571 E-5
AR	7.8769 E-6	8.1694 E-6	8.1562 E-6
TP	2.6719 E-4	2.6571 E-4	2.6330 E-4
SWEEP	2.8831 E-5	2.4199 E-5	2.6761 E-5

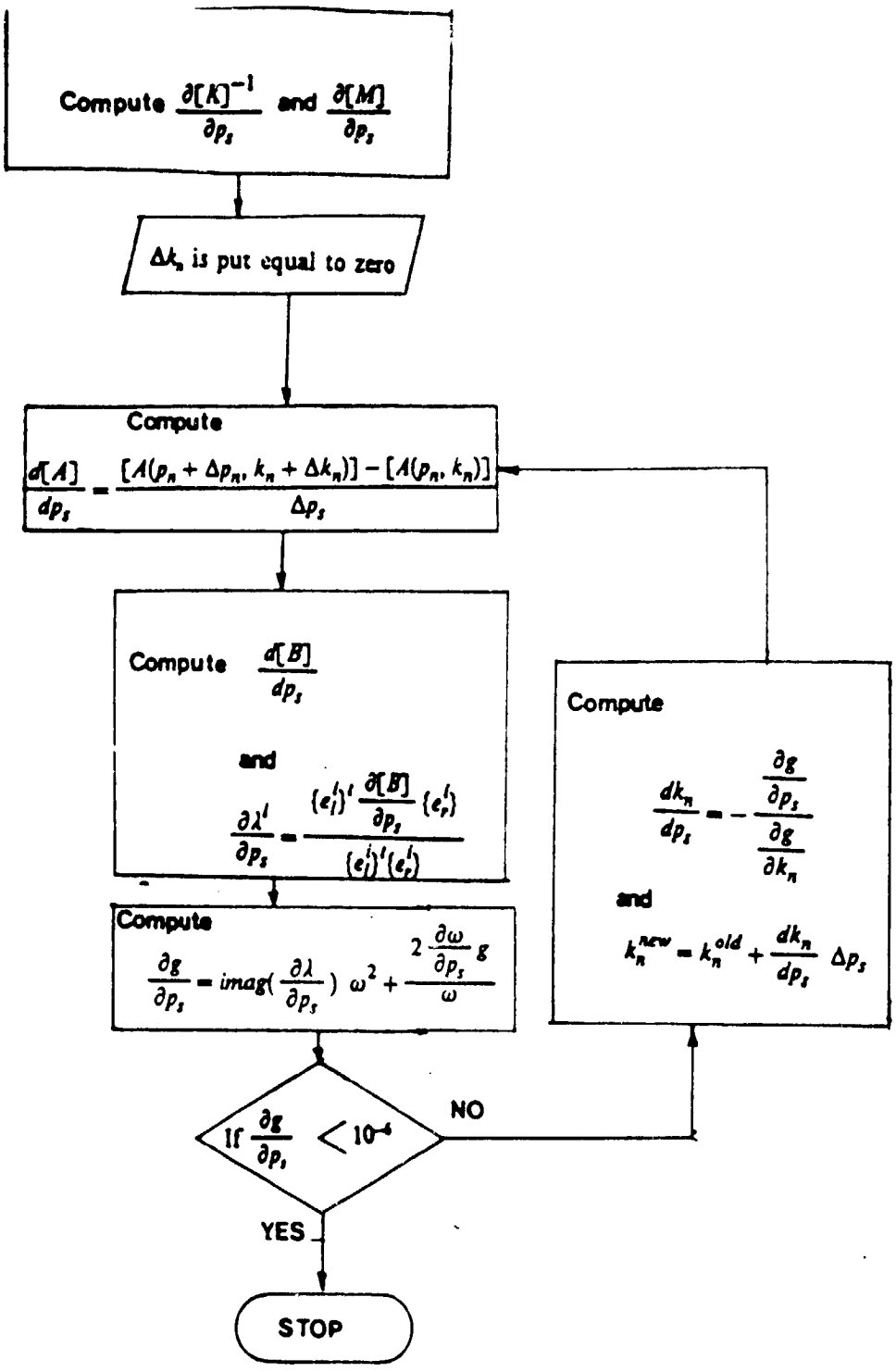

Figure 16 Flowchart for Semi-analytic Method

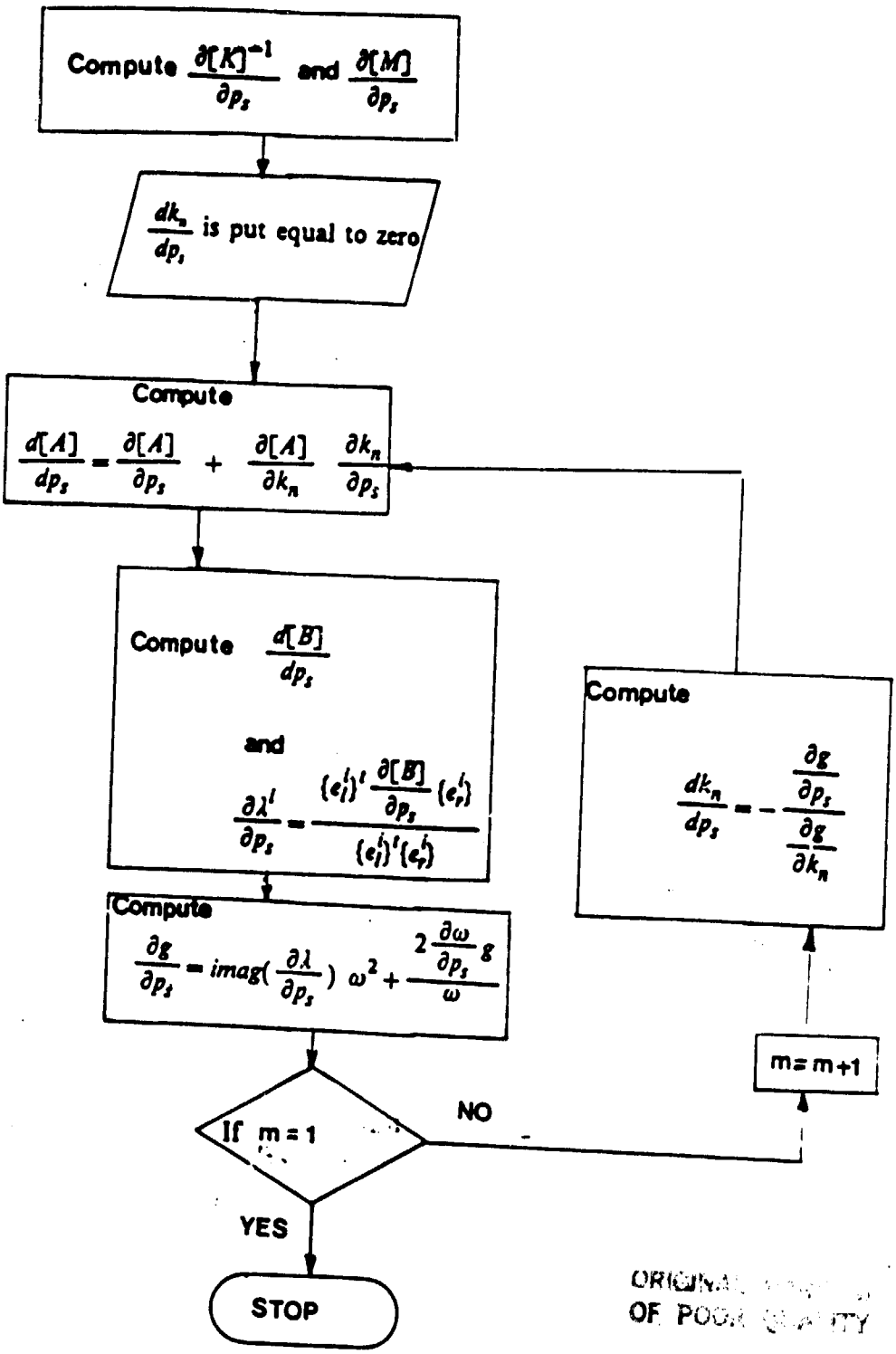

Figure 17 Flowchart for Analytic Method

Baseline: $S=20.0\ m^2$
AR=7.5
tp=.75
Sweep=0.0

Reanalysis
Sensitivity

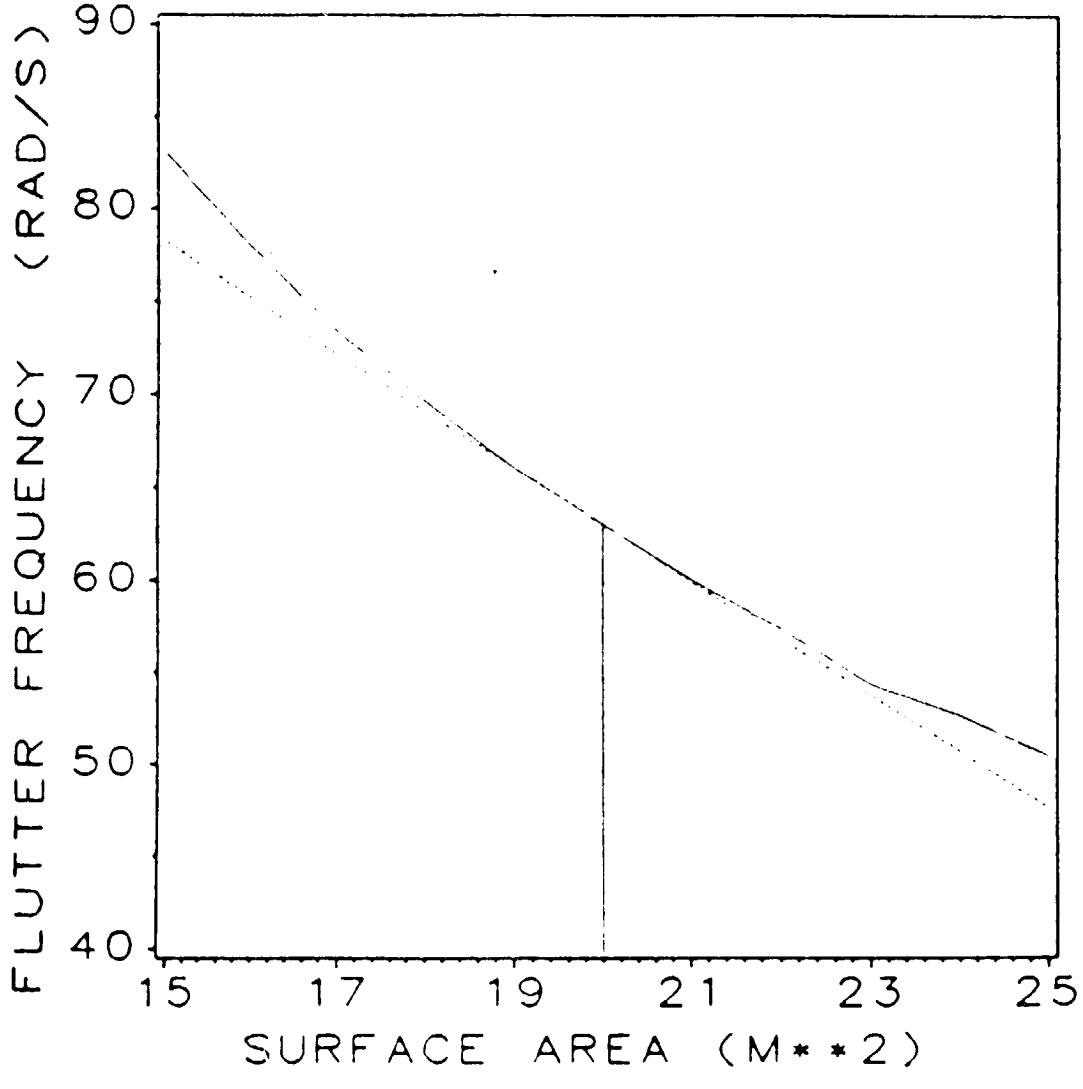

Figure 18 Flutter Frequency vs Surface Area

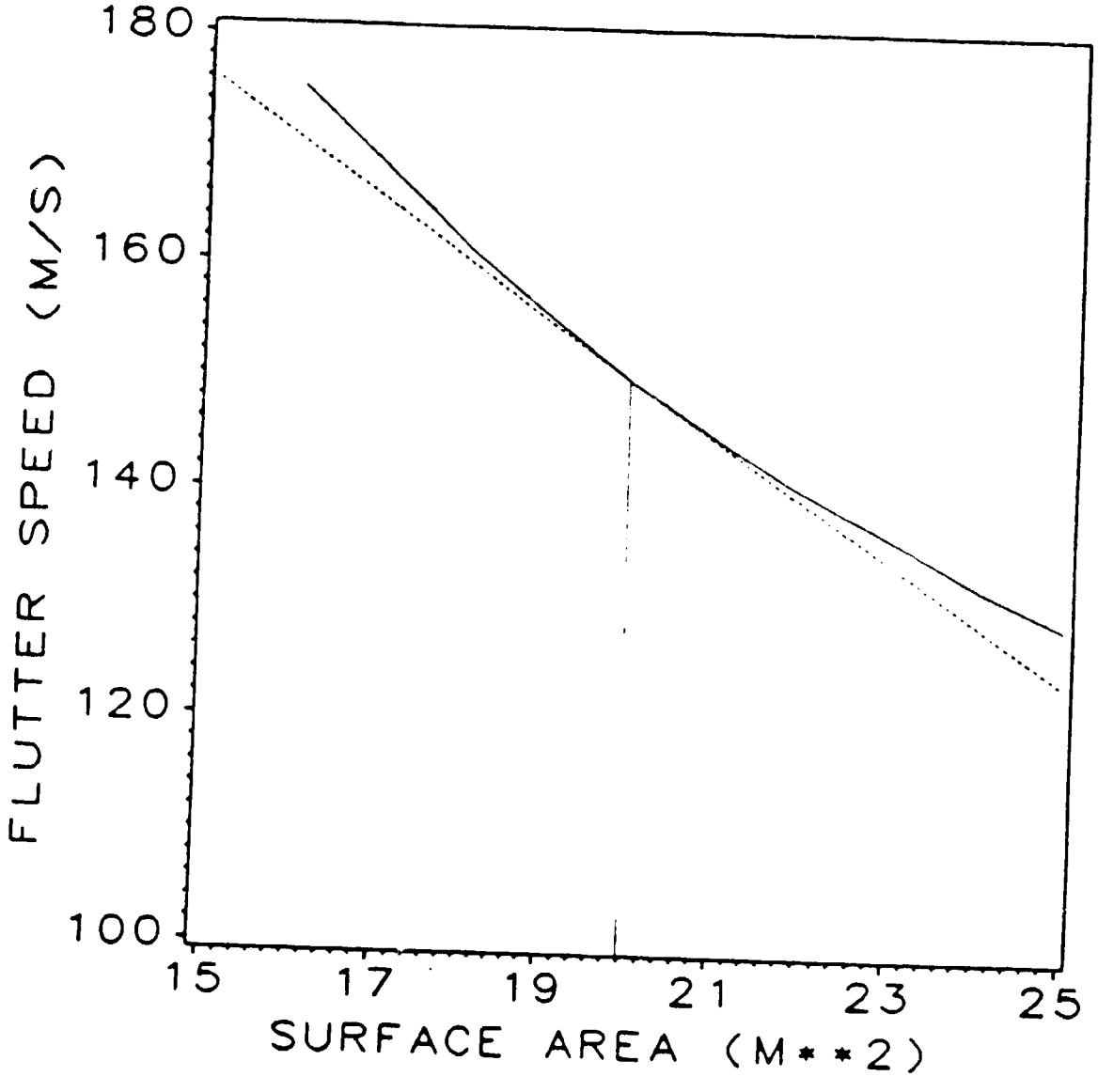

Figure 19 Flutter Speed vs Surface Area

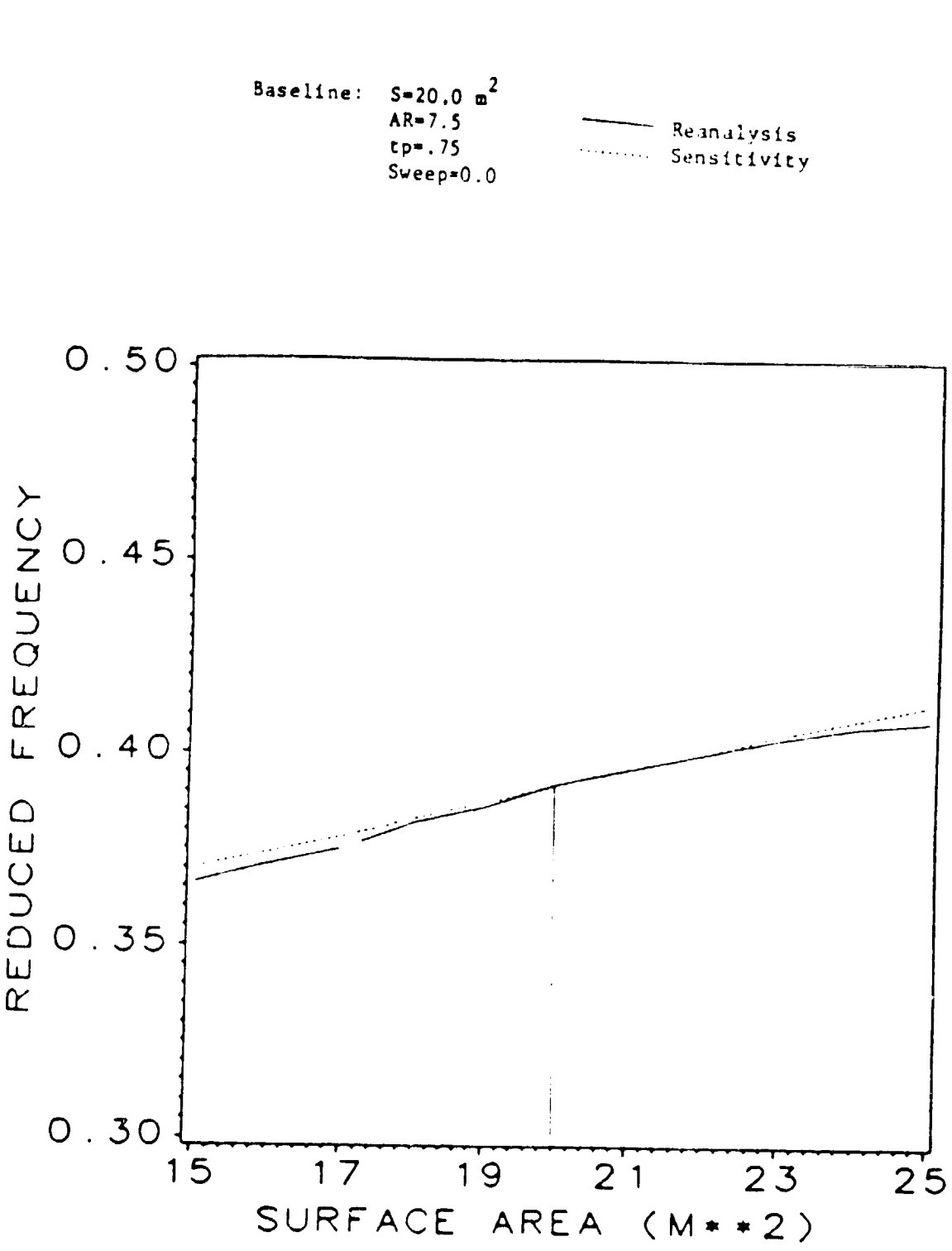

Figure 20 Reduced Frequency vs Surface Area

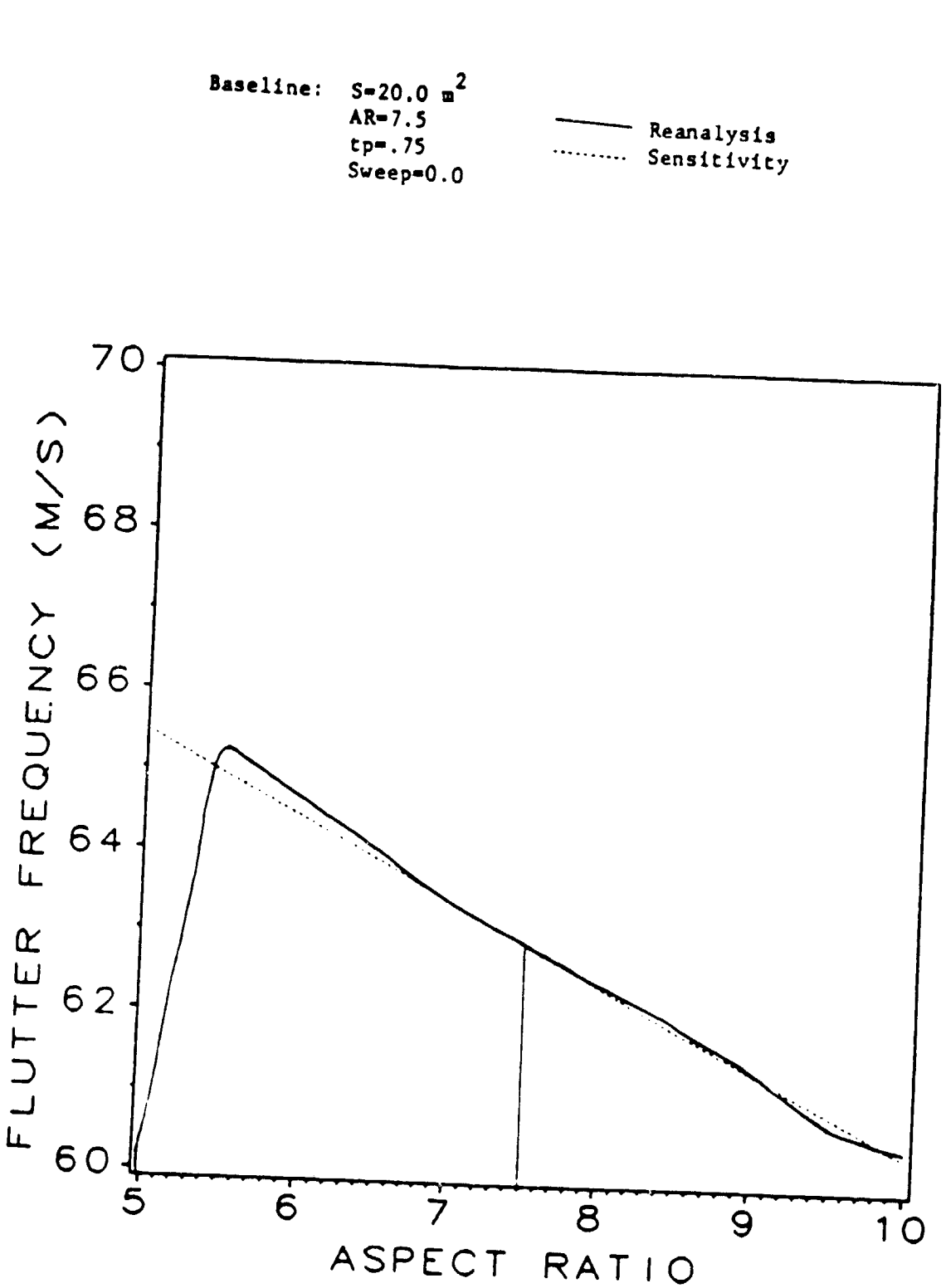

Figure 21 Flutter Frequency vs Aspect Ratio

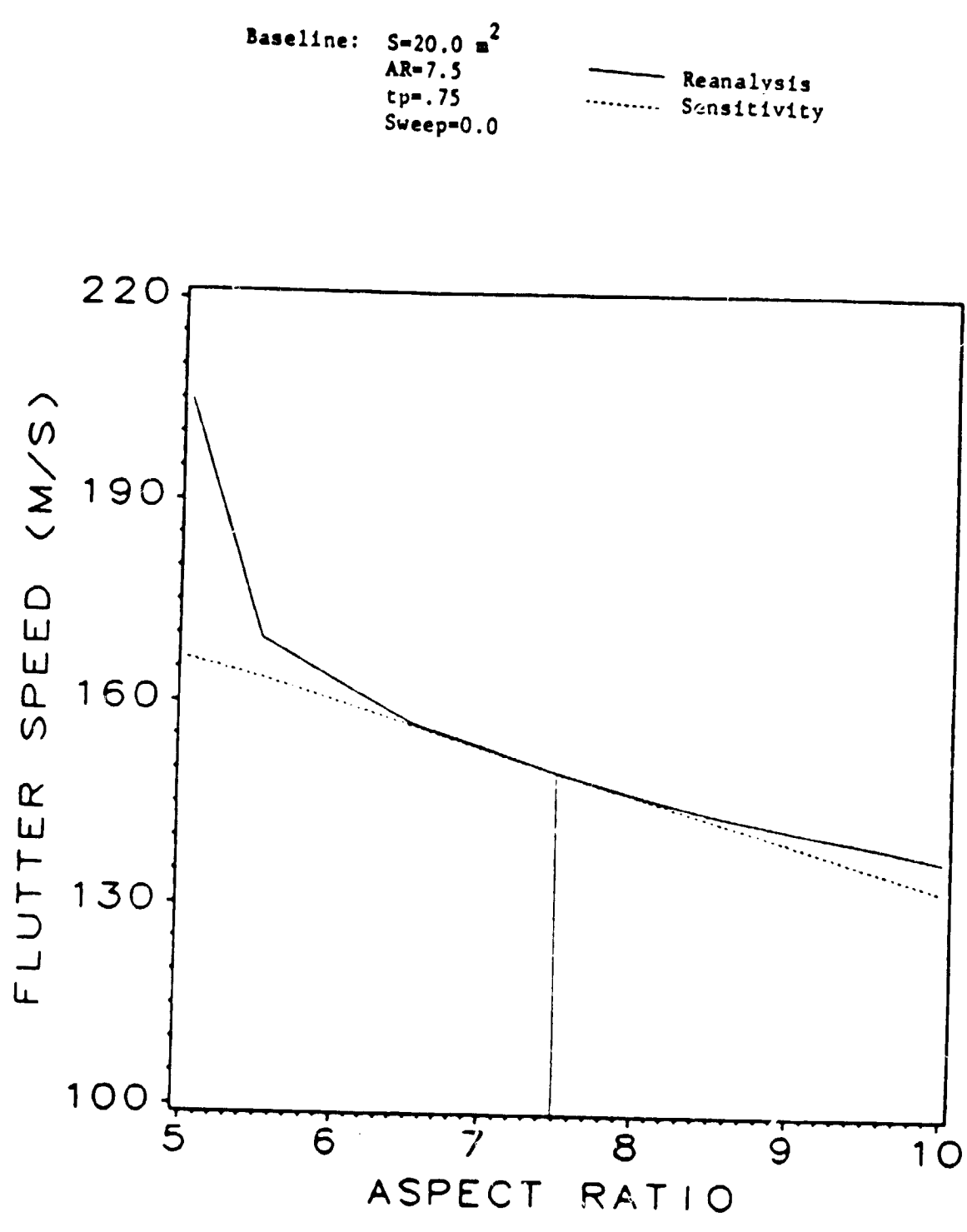

Figure 22 Flutter Speed vs Aspect Ratio

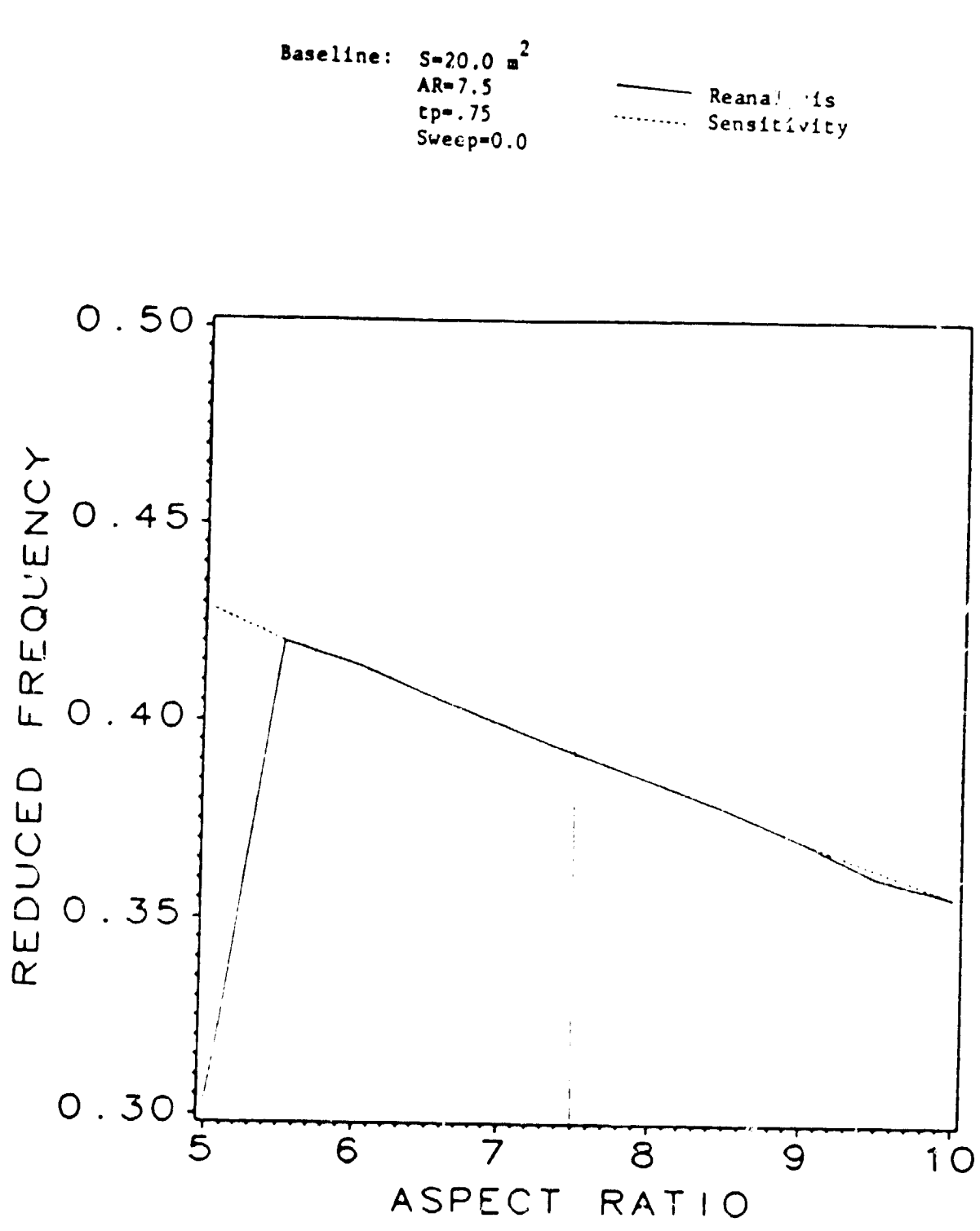

Figure 23 Reduced Frequency vs Aspect Ratio

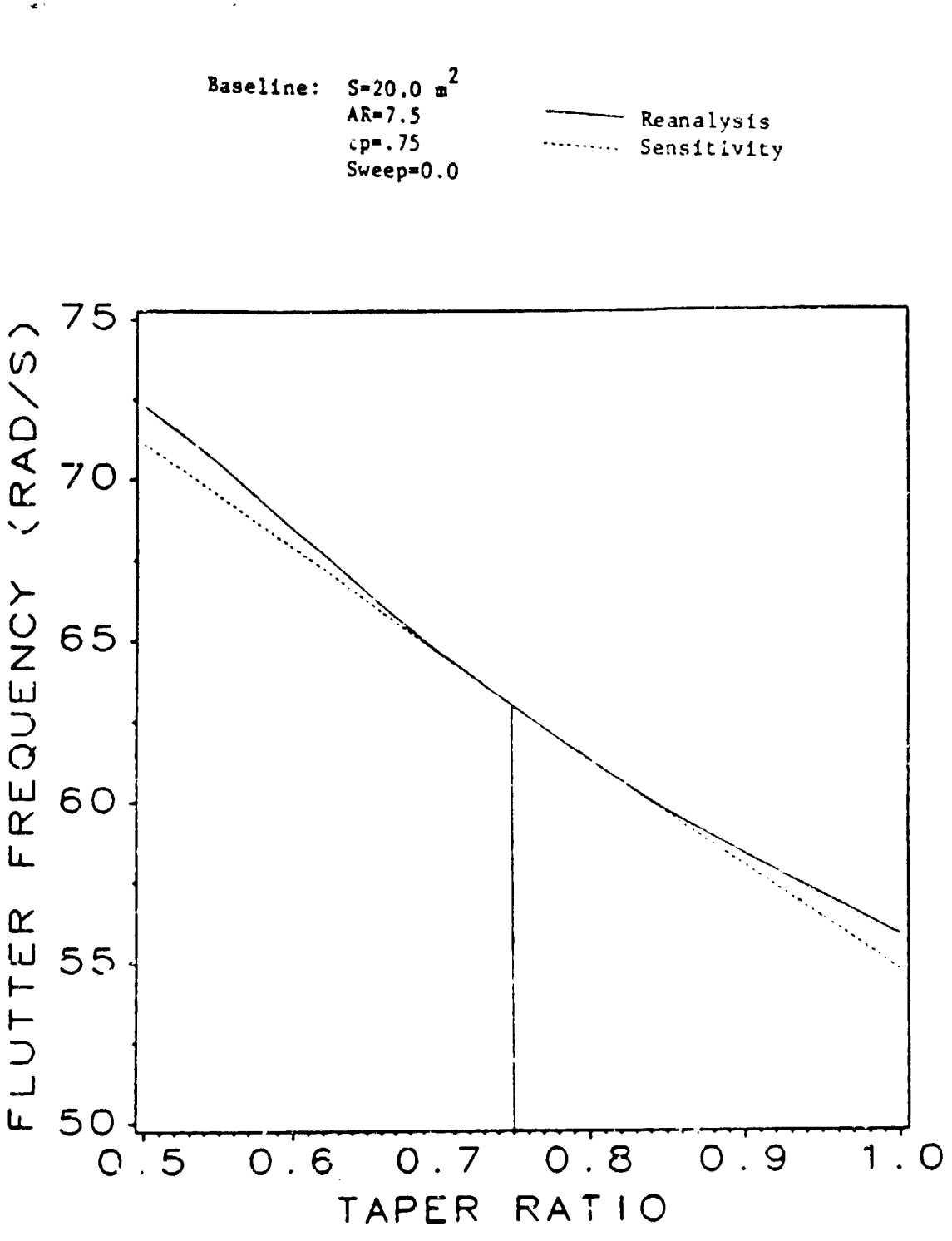

Figure 24 Flutter Frequency vs Taper Ratio

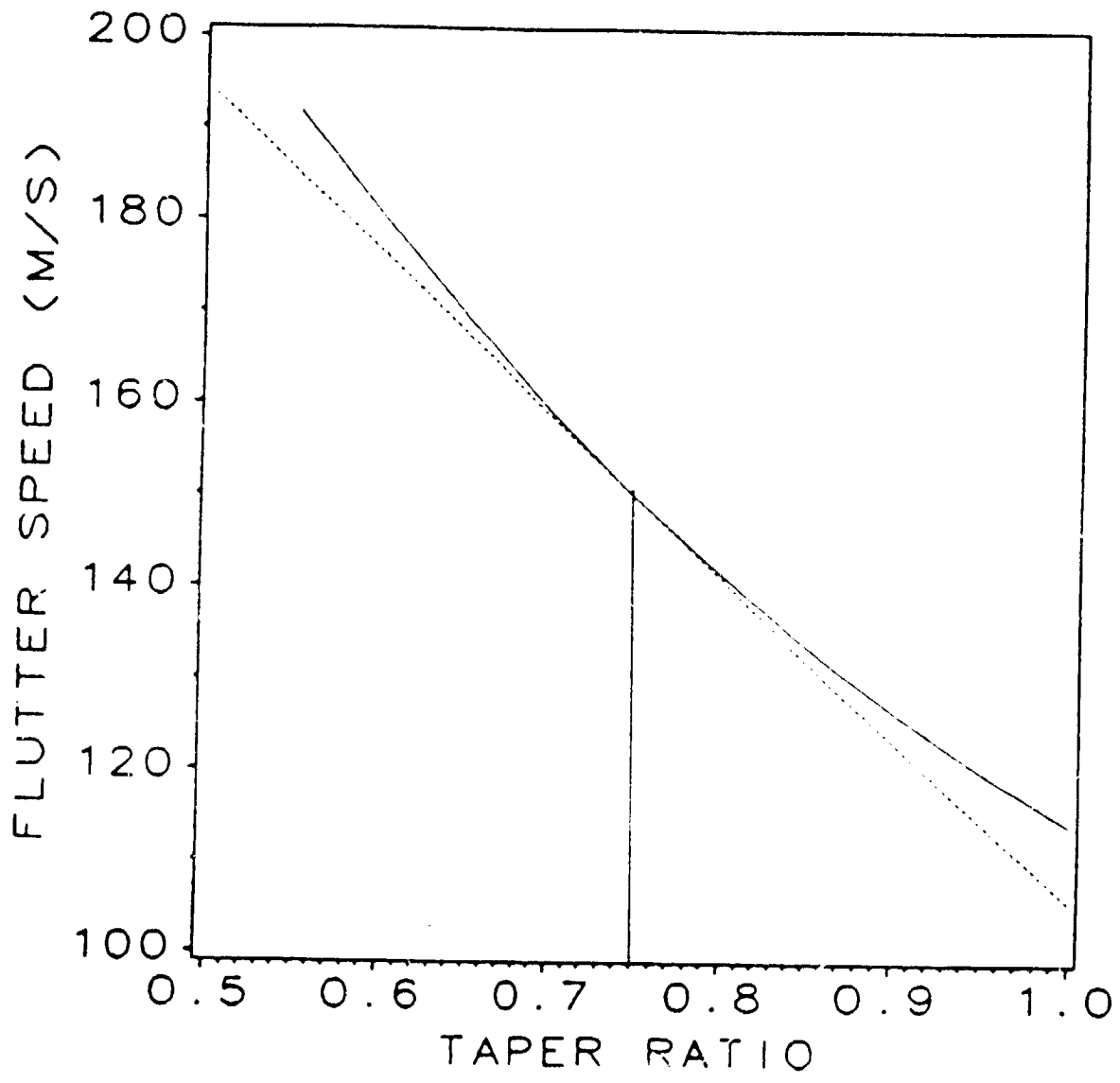

Figure 25 Flutter Speed vs Taper Ratio

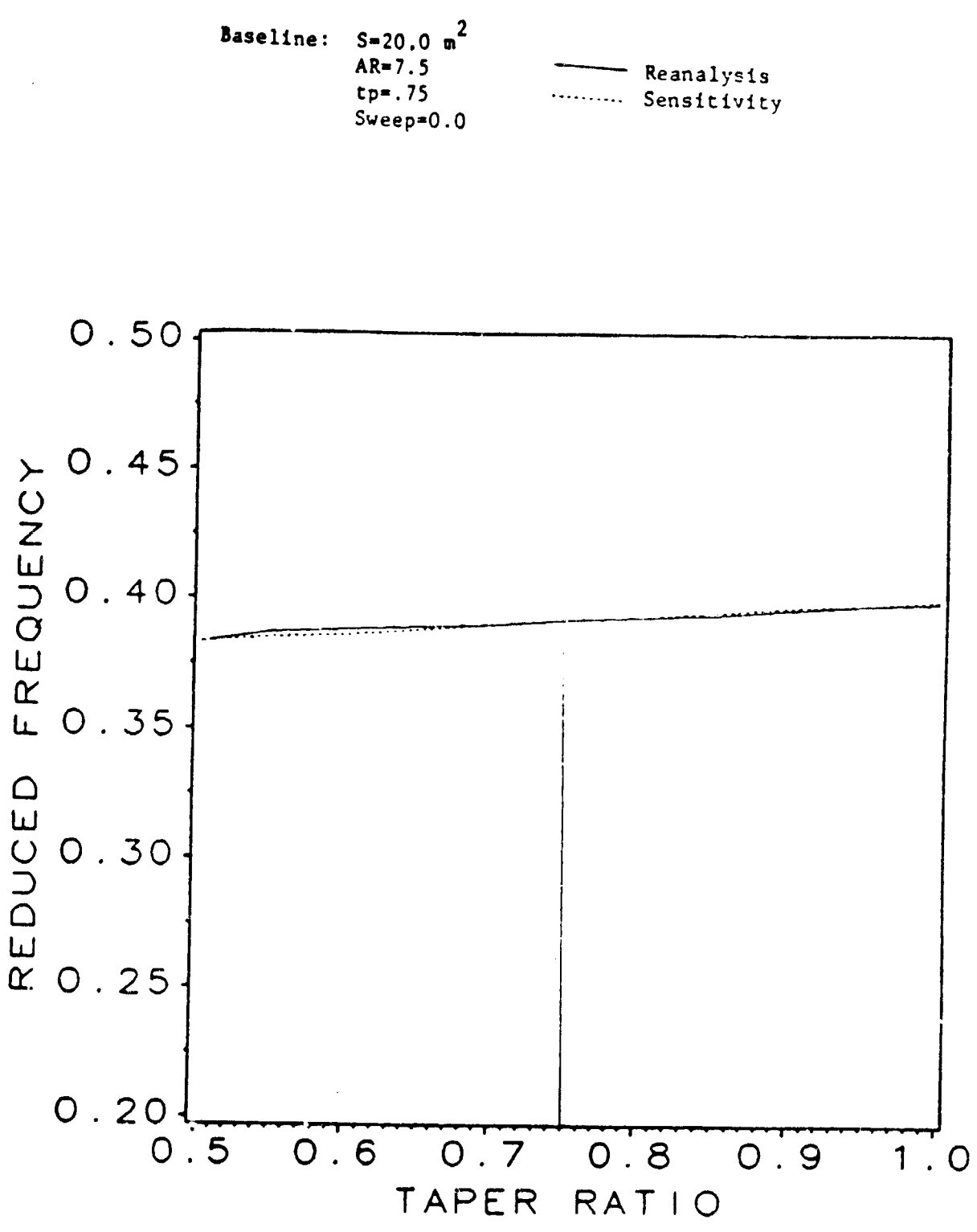

Figure 26 Reduced Frequency vs Taper Ratio

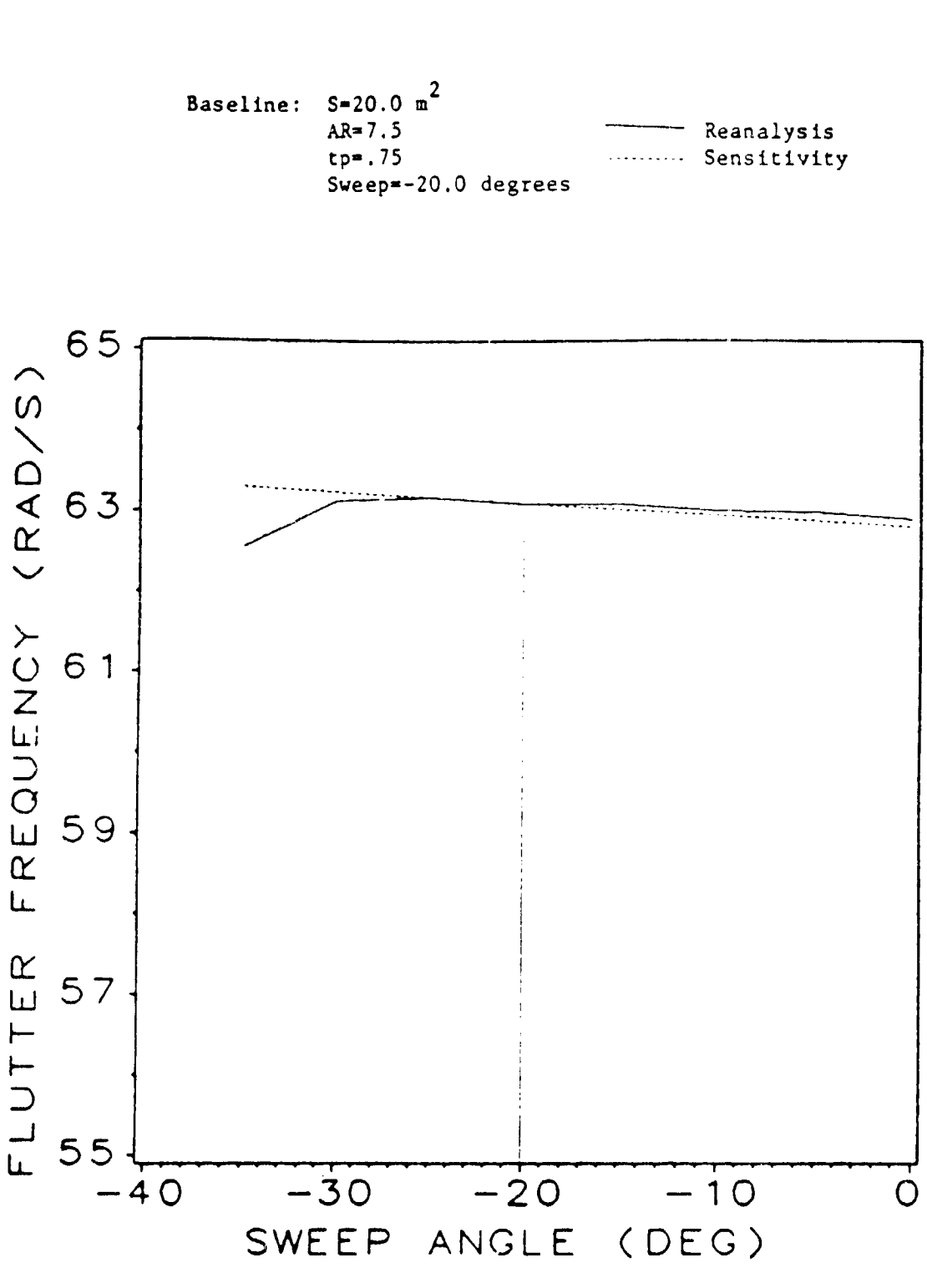

Figure 27 Flutter Frequency vs Sweep Angle

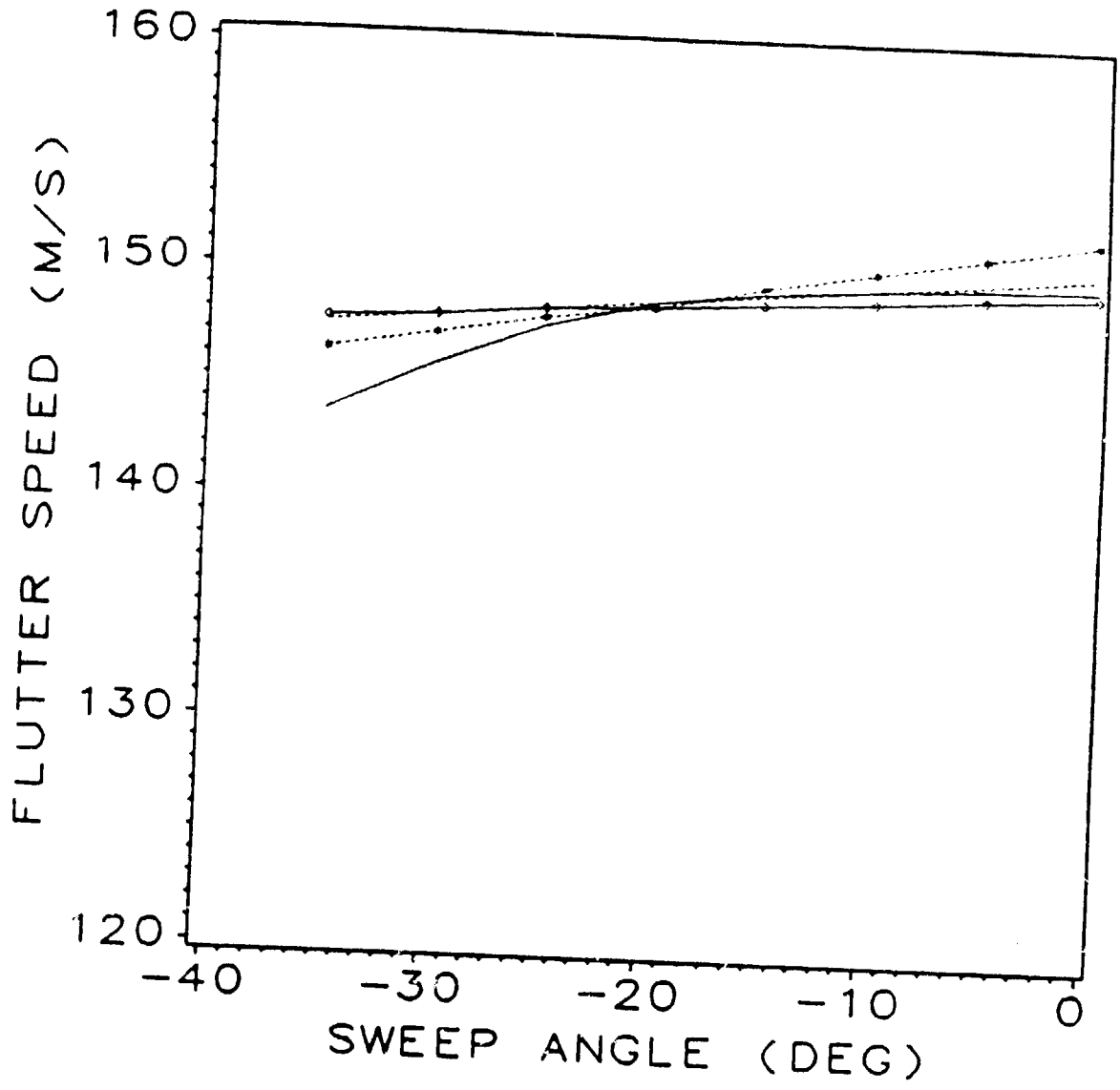

Figure 28 Flutter Speed vs Sweep Angle

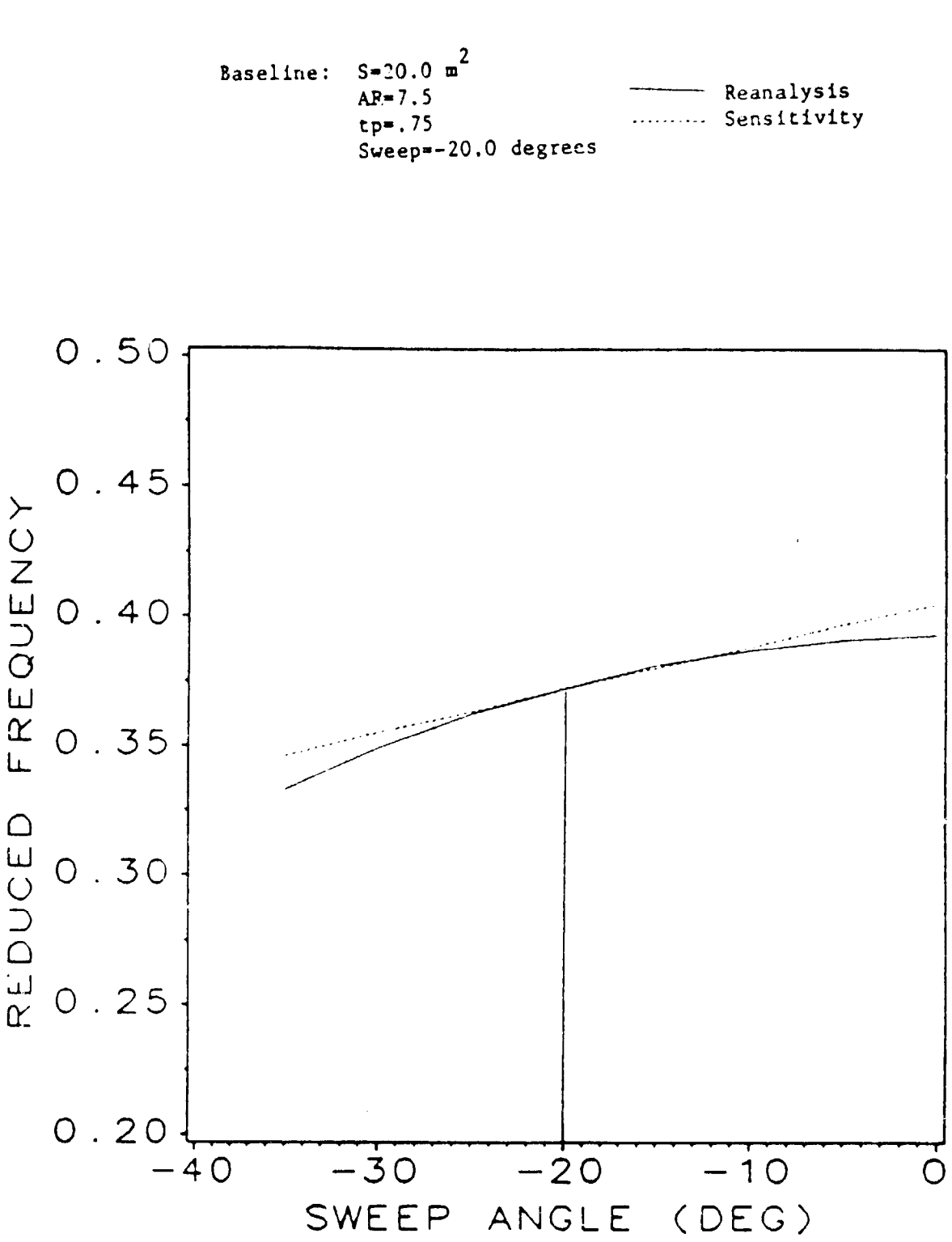

Figure 29 Reduced Frequency vs Sweep Angle

6.0 Conclusions and Suggestions for Future Work

A method for analyzing the dynamic aeroelastic behavior of a laminated wing has been developed. The aerodynamic formulation was taken from Yates' modified finite strip method. This was combined with Giles' equilavent plate model which is capable of analyzing cranked wing box structures. Three different approaches were used to obtain the sensitivity of the flutter speed, frequency, and reduced frequency. The first was a purley numerical approach using finite difference method. The second used the analytic expressions for the derivative of the eigenvalue as originally derived by Lancaster [19], and a finite difference method to the calculate the derivatives of the aerodynamic, mass and stiffness matrices. The third method also used Lancaster's [19] expression for the eigenvalue derivative but the derivative of the aerodynamic matrix is computed analytically.

It was shown that the eigenvalue derivatives for all three cases are in good agreement with each other. Also the results for flutter speed and reduced frequency obtained using sensitivity based analysis, for a significant range of parameters, are found to be in good agreement with those obtained using a complete reanalysis.

There is ample room for additional work in the area of Aerodynamic sensitivity analysis. This work can be extended to include the analytical derivatives of the mass and stiffness matrices. This will eleminate any uncertainties in choosing a finite difference step size and be of great use to the present optimization codes.

An improved aerodynamic code could be added to include the effect of chordwise bending of the box structure. This can be achieved by using the aerodynamic coefficients developed by Spielberg [26] to modify the present analysis.

The variation of the curvature of the flutter speed, flutter frequency , and reduced frequency could be predicted more acurately by a second order derivative. For a general complex matrix, efficient calculations of these derivatives are present by Murthy and Haftka [19].

The aerodynamic sensitivity calculations of a wing with mass stores is needed in the industry. The changing mass configurations of a wing with missiles and bombs is a typical example for the need of such an analysis capability.

This work can be extended to include the sensitivities of the flutter speed, flutter frequency, and reduced frequency to a simultaneous change in several shape parameters. For example, the sensitivity of flutter speed with the changes in sweep and aspect ratio would be useful. The structural code used in this analysis is extremely versatile and can be extended with the present aerodynamic formulation to analyze cranked wing boxes.

7.0 References

1. Bisplinghoff, R. L., Ashley, H., and Halfman, R. L., *Aeroelasticity*, Addison-Wesley Publishing Company, Inc., Reading, Mass. 1955.

2. Loring, S. J., "General Approach to the Flutter Problem", *S.A.E. Transactions*, Vol. 49, Aug.,1941, pp.345-356.

3. Yates E. C.,"Calculation of Flutter Characteristics for Finite-Span Swept or Unswept Wings at Subsonic and Supersonic Speeds by a Modified Strip Analysis", NACA RM L57110, March 18 1958 (Declassified Feb. 6, 1962)

4. Landsberger, B. J., and Dugundji, J.,"Experimental Aeroelastic Behavior of Unswept and Forward-Swept Cantilever Graphite/Epoxy Wings", *Journal of Aircraft*, Vol.22, No.8, August 1985.

5. Spielberg, I.N., "The Two-Dimensional Incompressible Aerodynamic Coefficients for Oscillatory Changes in Airfoil Camber", *Journal of the Aeronautical Sciences*, Vol.20, June 1953, pp.389-396.

6. Strganac, T. W., and Mook D. T.,"A New Method to Predict Unsteady Aeroelastic Behavior", *AIAA 28th Structures, Structural Dynamics and Materials Conference* April 6-8 1987.

7. Waldman, W., "A Fortran Program for the Determination of Unsteady Airforces on General Combinations of Interfering Lifting Surfaces Oscillating in Subsonic Flow", Structures Report 412 D.O.D. of Australia., January 1985.

8. Hawk, D. J., and Bristow, D. R., 1984: "Development of MCAERO Wing Design Panel Method With Interactive Graphics Module", NASA CR-3775.

9. Brayton, R. K., and Spence, R.,*Sensitivity and Optimization* ,Elsevier, New York, 1980.

10. Frank, P. M.,*Introduction to Sensitivity Theory*, Academic Press, Orlando, Fl., 1978.

11. Radanovic, L. (ed.),"Sensitivity Methods in Control Theory", Pergamon Press, Oxford, England, 1966.

12. Tomovic, R.,"Sensitivity Analysis of Dynamic Ststems", Mcgraw-Hill Book Co., New York, 1963.

13. Adelman, H. M., and Haftka, R. T., "Sensitivty Analysis of Discrete Structural Systems", *AIAA Journal* , Vol. 24, No.5, May 1986, pp.823-831.

14. Rudisill, C. S., and Bhatia K. G.,"Optimization of Complex Structures to Satisfy Flutter Requirements", *AIAA Journal* ,Vol.9, No.8, August 1971, pp.1486-1491.

15. Pedersen, P and Seyranian, A. P.,"Sensitivity Analysis for Problems of Dynamic Stability", *International Journal of Solids and Structures*,Vol. 19, No.4, 1983, pp.315-335.

16. Yates, E. C., "Aerodynamic Sensitivity from Subsonic, Sonic, and Supersonic Unsteady, Nonplanar Lifting Surface Theory" NASA TM-100502, 1987.

17. Barthelemy, J-F. M., and Bergen, F. D., "Shape Sensitivity Analysis of Wing Static Aeroelastic Characteristics",NASA TP-2808, May 1988.

18. Giles, G. L.,"Equivalent Plate Analysis of Aircraft Wing Box Structures with General Planform Geometry", NASA TM 87697, March 1986

19. Murthy D. V., and Haftka, R. T.,"Derivatives of Eigenvalues and Eigenvectors of a General Complex Matrix", *Department of Aerospace and Ocean Engineering, VPI&SU* , June 1986

20. Barmby, J. G., Cunningham, H. J., and Garrick, I. E.,"Study of Effects of Sweep on the Flutter of Cantilever Wings", *NACA TN 2121*, June 1950.

21. Castel, F. , and Kapania, R., "A Beam Element for the Aeroelastic Analysis of Undamaged and Damaged Laminated Structures", *CCMS Report*, July 1988.

22. Beer, F. P., and Johnston, R. E., *Mechanics of Materials*, 1st ed., Vol. 1, McGraw-Hill, New York, 1981, p.598.

23. Carnahan, B., Luther, H. A., and Wilkes, J. O., *Applied Numerical Methods*, 1st ed., Vol. 1, Wiley, New York, 1969, p.103.

24. Fung, Y. C.,*An Introduction to the Theory of Aeroelasticity* , Dover Publications, Inc., New York, 1945 pp.215-241.

25. Craig, R. R.,*Structural Dynamics*,John Wiley and Sons, New York, 1981, p.215.

26. Deyoung, J., and Harper, C. W.," Theoretical Symmetric Span Loading Loading at Subsonic Speeds for Wings Having Aribitrary Plan Form", NACA Report No. 921, 1948.

27. Dowell, E. H., et al., *A Modern Course in Aeroelasticity*, Sijthoff & Noordhoff, Alphen aan den Rijn, The Netherlands, 1978, pp.72-100.

28. Goland, M.,"The Flutter of a Uniform Cantilever Wing", *Journal of Applied Mechanics*, December 1945 pp.197-208.

29. Haftka, R. T., and Yates, E. C.,"Repetitive Flutter Calculations in Structural Design", *Journal of Aircraft* , Vol.15, No.7, July 1976, pp.454-461.

30. Lottati, I.,"Flutter and Divergence Aeroelastic Characteristics for Composite Forward Swept Cantileverd Wing", *AIAA paper*, June 1985.

31. Meric, R. A.,"Shape Sensitivity Analysis of Dynamic Structures" , *AIAA Journal*, Vol.26, No.2, February 1988 pp.206-212.

32. Rao, S. S.,"Rates of Change of Flutter Mach Number and Flutter Frequency", *AIAA Journal*, Vol. 10, No.11, November 1972, pp.1526-1528.

33. Rudisill, C. S., and Bhatia K. G.,"Second Derivatives of the Flutter Velocity and the Optimization of Aircraft Structures", *AIAA Journal*,Vol.10, No.12, December 1972, pp.1569-1572.

34. Seyranian, A. P.,"Sensitivity Analysis and Optimization of Aeroelastic Stability", *International Journal of Solids and Structures*, Vol 18, No.9, pp 791-807, 1982.

35. Srinivasan, R. S., and Babu, B. J. C.," Free Vibration And Flutter of Laminated Quadrilateral Plates", *Computers and Structures* , Vol.27, No.2, November 1987 pp.303-312.

36. Theodorsen, T.,"General Theory of Aerodynamic Instability and the Mechanism of Flutter" NACA Report No.496, May 1934.

NASA National Aeronautics and Space Administration

Report Documentation Page

1. Report No.	2. Government Accession No.	3. Recipient's Catalog No.
NASA CR-181725		

4. Title and Subtitle

Shape Sensitivity Analysis of Flutter Response of a Laminated Wing

5. Report Date

October 1988

6. Performing Organization Code

7. Author(s)

Fred D. Bergen and Rakesh K. Kapania

8. Performing Organization Report No.

10. Work Unit No.

506-43-41-01

9. Performing Organization Name and Address

Virginia Polytechnic Institute & State University
Department of Aerospace and Ocean Engineering
Blacksburg, VA 24061

11. Contract or Grant No.

NAS1-18471 - Task 5

12. Sponsoring Agency Name and Address

National Aeronautics and Space Administration
Langley Research Center
Hampton, VA 23665-5225

13. Type of Report and Period Covered

Contractor Report

14. Sponsoring Agency Code

15. Supplementary Notes

Langley Technical Monitor: J-F M. Barthelemy

16. Abstract

A method is presented for calculating the shape sensitivity of a wing aeroelastic response with respect to changes in geometric shape. Yates' modified strip method is used in conjunction with Giles' equivalent plate analysis to predict the flutter speed, frequency, and reduced frequency of the wing. Three methods are used to calculate the sensitivity of the eigenvalue. The first method is purely a finite difference calculation of the eigenvalue derivative directly from the solution of the flutter problem corresponding to the two different values of the shape parameters. The second method uses an analytic expression for the eigenvalue sensitivities of a general complex matrix, where the derivatives of the aerodynamic, mass, and stiffness matrices are computed using a finite difference approximation. The third method also uses an analytic expression for the eigenvalue sensitivities, but the aerodynamic matrix is computed analytically. All three methods are found to be in good agreement with each other. The sensitivities of the eigenvalues were used to predict flutter speed, frequency, and reduced frequency. These approximations were found to be in good agreement with those obtained using a complete reanalysis. However, it is recommended that higher order terms be used in the calculations in order to assure greater accuracy.

17. Key Words (Suggested by Author(s))	18. Distribution Statement
Sensitivity analysis Flutter Composites	Unclassified - Unlimited Subject Category 05,34,39

19. Security Classif. (of this report)	20. Security Classif. (of this page)	21. No. of pages	22. Price
Unclassified	Unclassified	95	A05

NASA FORM 1626 OCT 86